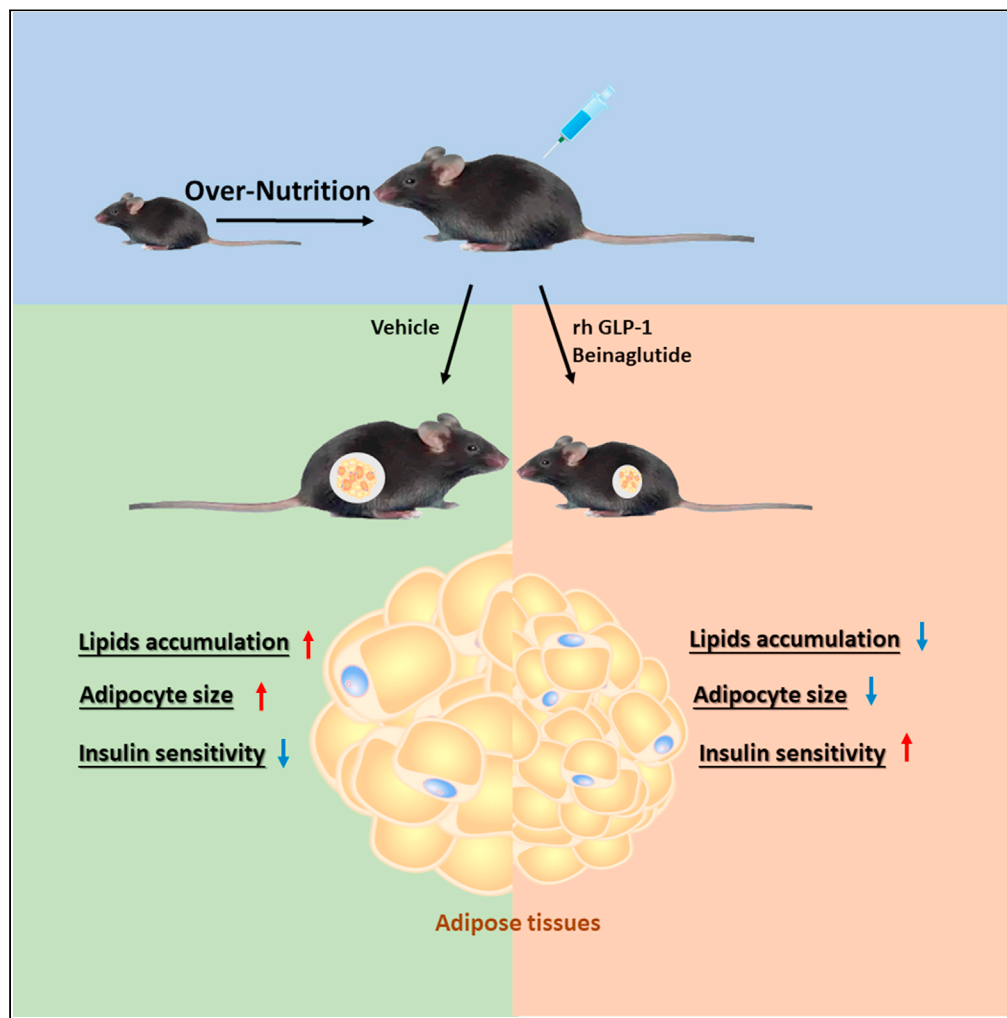


Article

# Recombinant human GLP-1 beinaglutide regulates lipid metabolism of adipose tissues in diet-induced obese mice



Feng Zhang,  
Zhinan Chen, Dan  
Wu, ..., Zhiguang  
Zhou, Zhiqiang  
Du, Fang Hu

zdu2005@163.com (Z.D.)  
hu\_fang98@csu.edu.cn (F.H.)

**Highlights**

Recombinant human GLP-1 Beinaglutide (BN) reduces high-fat-diet-induced obesity

BN increases insulin sensitivity of adipocytes *in vivo* and *in vitro*

BN alters lipidomic and transcriptomic profiles in adipose tissues of obese mice

BN promotes thermogenic gene expression in adipose tissues

Zhang et al., iScience 24, 103382  
December 17, 2021 © 2021 The Authors.  
<https://doi.org/10.1016/j.isci.2021.103382>



## Article

## Recombinant human GLP-1 beinaglutide regulates lipid metabolism of adipose tissues in diet-induced obese mice

Feng Zhang,<sup>1</sup> Zhinan Chen,<sup>1</sup> Dan Wu,<sup>1</sup> Le Tian,<sup>1</sup> Qing Chen,<sup>1</sup> Yuqing Ye,<sup>1</sup> Wei Chen,<sup>1</sup> Xiaoxing Wu,<sup>2</sup> Peng Wu,<sup>2</sup> Weilan Yuan,<sup>2</sup> Yan Qiu,<sup>2</sup> Zhiguang Zhou,<sup>1</sup> Zhiqiang Du,<sup>2,\*</sup> and Fang Hu<sup>1,3,\*</sup>

## SUMMARY

**GLP-1 analogs are a class of glucose-lowering agents with multiple benefits in diabetes, but its role in adipose tissues remains to be elucidated. The aim of this study was to determine the action of recombinant human GLP-1 (rhGLP-1) Beinaglutide (BN) in the insulin sensitivity and lipid metabolism of adipose tissues. We have shown that, after BN injection, obese mice displayed lower body weight, fat mass, and plasma lipid levels. In addition, BN promoted the insulin sensitivity in the white adipose tissues. Furthermore, we have found that the BN treatment caused significant changes in content and composition of different lipid classes, including glycerolipids, glycerophospholipids, and sphingolipids, as well as expression of genes in lipid metabolic pathways in the adipose tissues. Taken together, our data demonstrate that BN could resist HFD-induced obesity by targeting the composition of major lipid classes and the expression of genes in lipid metabolism of adipose tissues.**

## INTRODUCTION

Over the past 50 years, obesity has become a major worldwide health problem because it increases the risk of type 2 diabetes (T2DM), heart disease, fatty liver disease, stroke, cancer, and many other diseases greatly, leading to a decline in expectancy and quality of life (Bluher, 2019; Danaei et al., 2011). Although there are some anti-obesity drug candidates, they have limited efficacy and/or cause unacceptable adverse effects (Adan, 2013; Scheen and Van Gaal, 2014).

Glucagon-like peptide-1 (GLP-1), encoded by the proglucagon gene, is a peptide that is mainly secreted from L cells in the small and large intestine and from neurons in the nucleus tractus solitarius (NTS) of the caudal brain stem (Drucker, 2018). As a potent incretin hormone, GLP-1, has multi-tissue protective effects, and its analogs are widely used as pharmacological therapies for T2DM and associated diseases. In the pancreas, GLP-1 stimulates insulin secretion and inhibits glucagon secretion, protects against beta-cell apoptosis, and promotes cell proliferation (Doyle and Egan, 2007). GLP-1 displays cardioprotective effects through direct activation of antiapoptotic mechanisms in cardiomyocytes (Noyan-Ashraf et al., 2009). In the liver, GLP-1 promotes hepatic glucose uptake and increases glycogen production by stimulating glycogen synthase activity (D'Alessio et al., 2004).

Although the circulating level of endogenous GLP-1 rises rapidly within minutes of food intake (Orskov et al., 1996), it is rapidly degraded by the enzyme dipeptidyl peptidase-4 (DPP-4) to inactive metabolites and, therefore, has a short circulating half-life of several minutes (Vilsboll et al., 2003). A number of GLP-1 analogs have been developed and can be classified as either short-acting or long-acting compounds according to their pharmacokinetic characteristics. The short-acting GLP analogs (such as exenatide and lixisenatide) are characterized by large-amplitude fluctuations in plasma peptide levels when administered at typical intervals (Kolterman et al., 2003). The long-acting compounds (such as albiglutide, dulaglutide, exenatide long-acting release, and liraglutide), at their typical administration intervals, lead to a more consistent, supraphysiological activation of the GLP-1 receptor (GLP-1R) (Agersù et al., 2002; Drucker et al., 2008). These pharmacokinetic differences between short- and long-acting reagents may cause differences in action, efficacy, and tolerability of these compounds in the application. For example, short-acting GLP-1 analogs mainly lower postprandial glucose levels and insulin concentrations via

<sup>1</sup>National Clinical Research Center for Metabolic Diseases, Key Laboratory of Diabetes Immunology, Ministry of Education, Metabolic Syndrome Research Center, Department of Metabolism and Endocrinology, The Second Xiangya Hospital of Central South University, Changsha, 410011 Hunan, China

<sup>2</sup>Innovation Center, Shanghai Benemae Pharmaceutical Corporation, 916 Ziping Road, PuDong, Shanghai, China

<sup>3</sup>Lead contact

\*Correspondence: zdu2005@163.com (Z.D.), hu\_fang98@csu.edu.cn (F.H.) <https://doi.org/10.1016/j.isci.2021.103382>



retardation of gastric emptying, whereas long-acting GLP-1 analogs lower blood glucose levels through stimulation of insulin secretion and reduction of glucagon levels (Alber et al., 2017; Lyseng-Williamson, 2019; Meier, 2012).

Besides glucose-lowering effects, GLP-1 analogs also reduce food intake and body weight in both human clinical trials and in experimental animal models (Elvert et al., 2018; Sun et al., 2015; Zhang et al., 2017). The GLP-1 analog liraglutide (trade name Saxenda) was approved by the Food and Drug Administration (FDA) in 2014 for weight loss treatment in obese individuals.

Apart from its effects on body weight and glucose, GLP-1 also acts as a regulator of lipid and lipoprotein metabolism. Acute and long-term treatment with either GLP-1 or its stable analogs reduced fasting as well as postprandial lipids in healthy and T2DM patients (Babenko et al., 2019; Svensson et al., 2019). Adipose tissues, including brown, beige, and classic white adipose tissues (WAT), play important roles in energy metabolism and body weight control and are also the major organs for lipid metabolism regulation. WAT are mainly responsible for fat storage, whereas brown adipose tissues (BAT) and beige adipocytes, mainly in subcutaneous white adipose tissues (SAT), control nonshivering thermogenesis or heat production by burning fat. Lipidome composition of the adipose tissues can be influenced by physiological factors such as adipocyte type, gender and age, or by environmental cues such as diets, thermal condition, and physical activity (Leiria and Tseng, 2020). The dynamic alterations in lipid composition play a pivotal role in the changes in tissue function, which are closely linked to whole-body energy metabolism. Lipidomic analyses of different adipose tissues performed recently under physiological (Hou et al., 2020), overnutrition (Caesar et al., 2010), or thermal stress (Marcher et al., 2015; Xu et al., 2019) conditions have provided valuable information about changes of lipid profiles of adipose tissues in response to various internal or external stimulators. Changes of lipidome profiles of adipose tissues in obesity and T2D have also been investigated (Al-Sulaiti et al., 2018). However, it is still unclear whether GLP-1 or its analogs have any effects on the lipidome of adipose tissues.

Beinaglutide (BN) is a recombinant human GLP-1 (rhGLP-1) that shares almost 100% homology with human GLP-1 (7–36). It is recommended for the treatment of T2DM by the Chinese Guideline for the Prevention and Treatment of Type 2 Diabetes (2017 edition). Clinical studies have shown that BN reduces body weight and body mass index (BMI) in overweight and obese T2DM patients (Zhang et al., 2019). Recently, pharmacological and pharmacokinetic profiles of BN were characterized, and its effects on nonalcoholic steatohepatitis (NASH) in animal models were reported (Fang et al., 2021). Acute and sub-chronic studies showed that repeated subcutaneous BN injection displays dose-dependent effects in glycemic control, inhibiting food intake and gastric empty and promoting weight loss. In this study, we aimed to determine the role of BN injection on adipose tissue insulin sensitivity and lipid metabolism. We have shown that HFD-induced obese mice treated with BN experienced reduced body weight and less fat accumulation in the adipose tissues. We have also shown that BN treatment increased adipocyte's insulin sensitivity *in vivo* and *in vitro*. More importantly, our mass-spectrometry-based lipidomics combined with RNA-seq analyses showed that BN treatment led to marked changes in the composition of lipids and the expression of genes involved in lipid metabolism in the adipose tissues, particular in the SAT. Our results provide evidence of the important role of rhGLP-1 BN in lipid metabolism and insulin activity in adipose tissues.

## RESULTS

### Beinaglutide-treated mice are lean and resistant to HFD-induced obesity and insulin resistance

To determine the role of rhGLP-1 in obese mice, we performed subcutaneous injections of BN to lean mice or HFD-induced obese mice for 6 weeks (Figure 1A). The frequency of BN administration (three times per day) and doses (150  $\mu$ g/kg/day) were selected according to efficacy of inhibiting food intake in a previous report, which has shown that BN inhibits food intake and gastric emptying in a dose-dependent manner in obese *ob/ob* mice (Fang et al., 2021). As expected, we observed significantly reduced (about 40%) daily food intake in the group of HFD-induced obese mice that were treated with BN but not in the lean mice (Figure 1B). The BN treatment significantly reduced the body weight (BW) of obese mice but not the lean mice. After 6 weeks of drug administration, the BW of obese mice was comparable to the same age lean mice fed with ND (Figures 1C and 1D). In the following studies, the HFD-induced obese mice treated with BN or Veh control were used for further analyses.

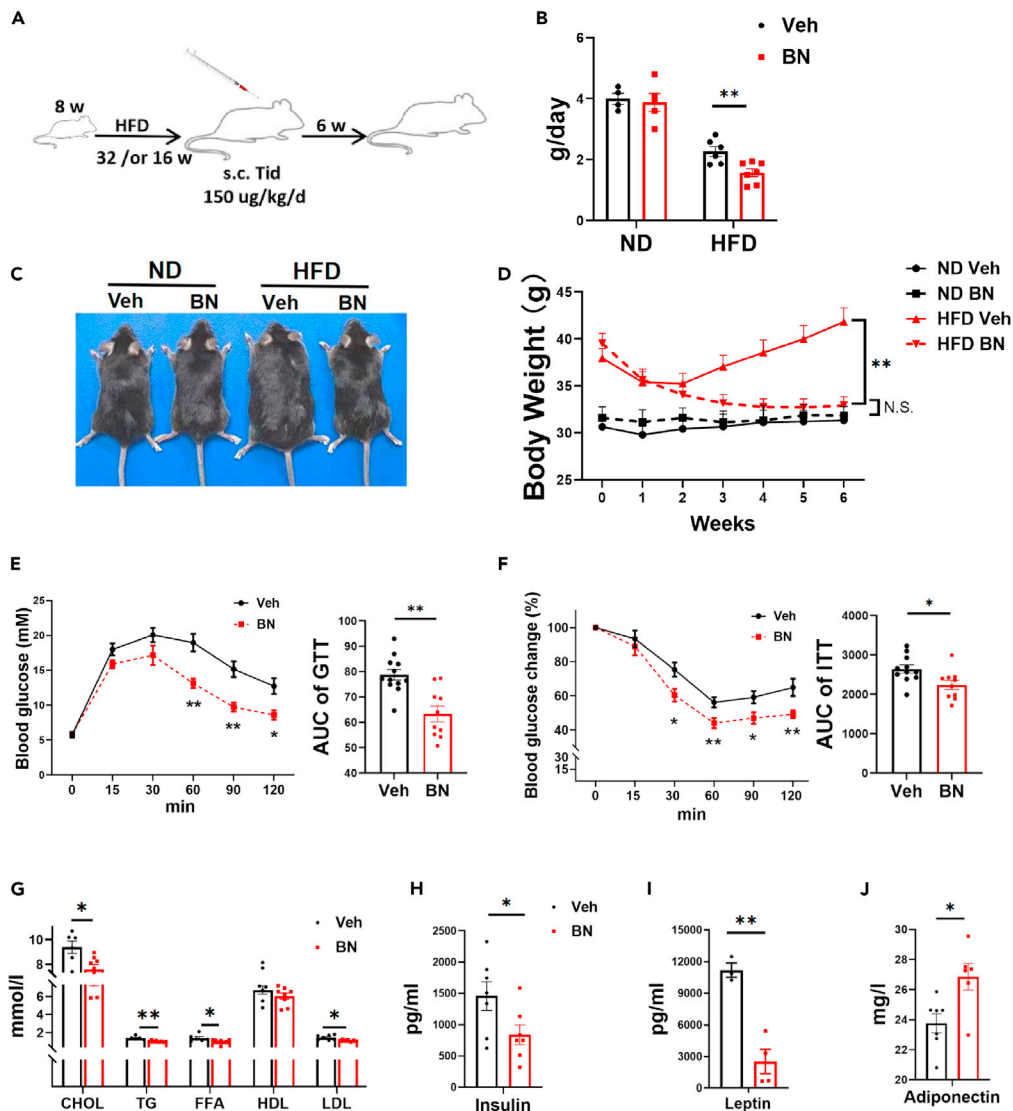


**Figure 1. Beinaglutide-treated mice are lean and resistant to HFD-induced obesity and insulin resistance**

(A) Eight-week-old male C57BL/6 mice were fed with a normal chow diet (ND) or high fat diet (HFD) for 16 or 32 weeks and then treated with recombinant human GLP-1 Beinaglutide (BN) or vehicle (Veh) control through subcutaneous injection for 6 weeks ( $n = 6-8$ /group).

(B) Average food intake of BN-treated or control mice.

(C) Representative images of lean and obese mice treated with BN or Veh.

(D) Body weight changes of lean and obese mice with 6-week BN or Veh treatment.

(E) Glucose tolerance test (GTT).

(F) Insulin tolerance test (ITT).

(G) Plasma levels of cholesterol (CHOL), triglyceride (TG), free fatty acid (FFA), high-density lipoprotein (HDL), and low-density lipoprotein (LDL).

(H–J) Plasma levels of insulin (H), leptin (I), and adiponectin (J).

Data were presented as mean  $\pm$  SEM. \* $p < 0.05$ ; \*\* $p < 0.01$  versus control. N.S, no significance

The results of glucose tolerance test (GTT) and insulin tolerance test (ITT) showed that BN-treated obese mice displayed improved glucose tolerance (Figure 1E) and insulin sensitivity (Figure 1F) compared with the control mice.

As individuals with obesity often display dyslipidemia, to determine the role of rhGLP-1 BN in plasma lipid levels in obese mice, we measured plasma free fatty acid (FFA), triglycerides (TG), and total cholesterol

(CHOL) from the HFD-induced obese mice treated with or without BN. The results showed that CHOL, TG, and FFA levels in the treated mice decreased significantly compared with the control mice (Figure 1G). In addition, plasma levels of low-density lipoprotein (LDL) in BN-treated obese mice also decreased, whereas high-density lipoprotein (HDL) levels were comparable between the two groups (Figure 1G). We also measured plasma levels of insulin, leptin, and adiponectin and found that insulin (Figure 1H) and leptin (Figure 1I) levels decreased significantly in the treated mice, suggesting that BN could reduce hyperinsulinemia and hyperleptinemia associated with obesity. Adiponectin, a fat-derived hormone, has multiple benefits on energy metabolism. Decrease in adiponectin levels are associated with obesity, diabetes, and cardiovascular diseases (Wang and Scherer, 2016). We found that plasma adiponectin level increased significantly (Figure 1J) in the treated mice, implying that BN has adiponectin-promoting effects.

### Beinaglutide treatment decreases adipose tissue weight and adipocyte size and potentiates insulin sensitivity of adipocytes *in vivo* and *in vitro*

In line with the reduced body weight, whole body fat (Figure 2A) as well as the interscapular BAT, inguinal SAT, and visceral white adipose tissues (VAT) (Figures 2B and 2C) of the treated mice were also significantly decreased.

Similar to those of the fats, the weight (Figure S2A) and the lipid droplet contents of the liver (Figure S2B) were significantly reduced in the treated mice. Ketone body  $\beta$ -hydroxybutyrate (BHB) is an important metabolite for energy supply and cellular signaling. We determined the blood BHB and found that BHB levels in the BN-treated obese mice significantly decreased compared with those of the control mice (Figure S2C).

Our data also showed that genes involved in lipolysis (e.g. *Pnpla2*) and lipogenesis (*Acc $\alpha$* , *Acc $\beta$* ) and genes involved in fatty acid oxidation (*Cpt1b*) were decreased in the liver (Figures S2D and S2E), which is in line with the reduced blood BHB levels. Ketogenesis occurs primarily in hepatic mitochondrial matrix at rates proportional to total fat oxidation. Decreased serum BHB levels and expression of genes involved in hepatic lipid metabolism and oxidation suggest overall reduced lipid metabolism in the liver of BN-treated mice.

We next measured sizes and numbers of adipocytes and found that BN administration significantly reduced numbers of large adipocytes ( $>25 \mu\text{m}$  in BAT,  $> 90 \mu\text{m}$  in WAT) whereas increased small adipocytes ( $<15 \mu\text{m}$  in BAT,  $< 80 \mu\text{m}$  in WAT) in the adipose tissues of obese mice (Figures 2D–2F).

As adipose tissues are important for insulin sensitivity, to determine the activity of insulin signaling in the presence of BN, we performed an intraperitoneal (i.p.) injection of insulin after BN administration and measured the activity of insulin-related signal molecules in the adipose tissues. The western blotting data showed that although BN treatment itself had no effects on insulin signaling activity, insulin-stimulated phosphorylation of Akt (both Thr308 and Ser473) was much higher in SAT (Figure 2G), but not in VAT (Figure 2H) and BAT (data not shown), of the BN-treated mice compared with those in the controls.

To determine whether BN has direct effects on insulin sensitivity in adipocytes, we treated 3T3-L1 cells with insulin alone or with BN. Consistent with what was observed in the SAT, BN treatment also potentiated insulin-stimulated phosphorylation of Akt in the adipocytes *in vitro* (Figure 2I). To further confirm these effects, we treated 3T3-L1 cells with insulin in the presence of GLP-1 and found that GLP-1 enhanced insulin signaling activity (Figure 2J). Taken together, our data suggest that GLP-1 and its analog rhGLP-1 BN can directly promote insulin sensitivity in the adipocytes.

### Beinaglutide treatment alters lipidomic profiles of adipose tissues

Lipids are the major constituents of the adipocytes, and the lipid composition of fat cells plays a critical role in maintaining cellular functions and communicating with other organs and cells. We analyzed lipidomics of adipose tissues treated with or without BN. The Q Exactive-based nontarget LC-MS analyses detected a total of 852 positive lipid species from 22 major lipid classes. The orthogonal projections to latent structures discriminant analysis (OPLS-DA) plot showed a clear separation pattern of the two groups in three adipose tissues (Figures S3A–S3C). Detected lipid classes and their abbreviations used throughout the paper are listed in Table S1. Among the lipid classes, TG, phosphatidylethanolamines (PE), and phosphatidylcholine (PC) were the most abundant lipids that were altered by BN

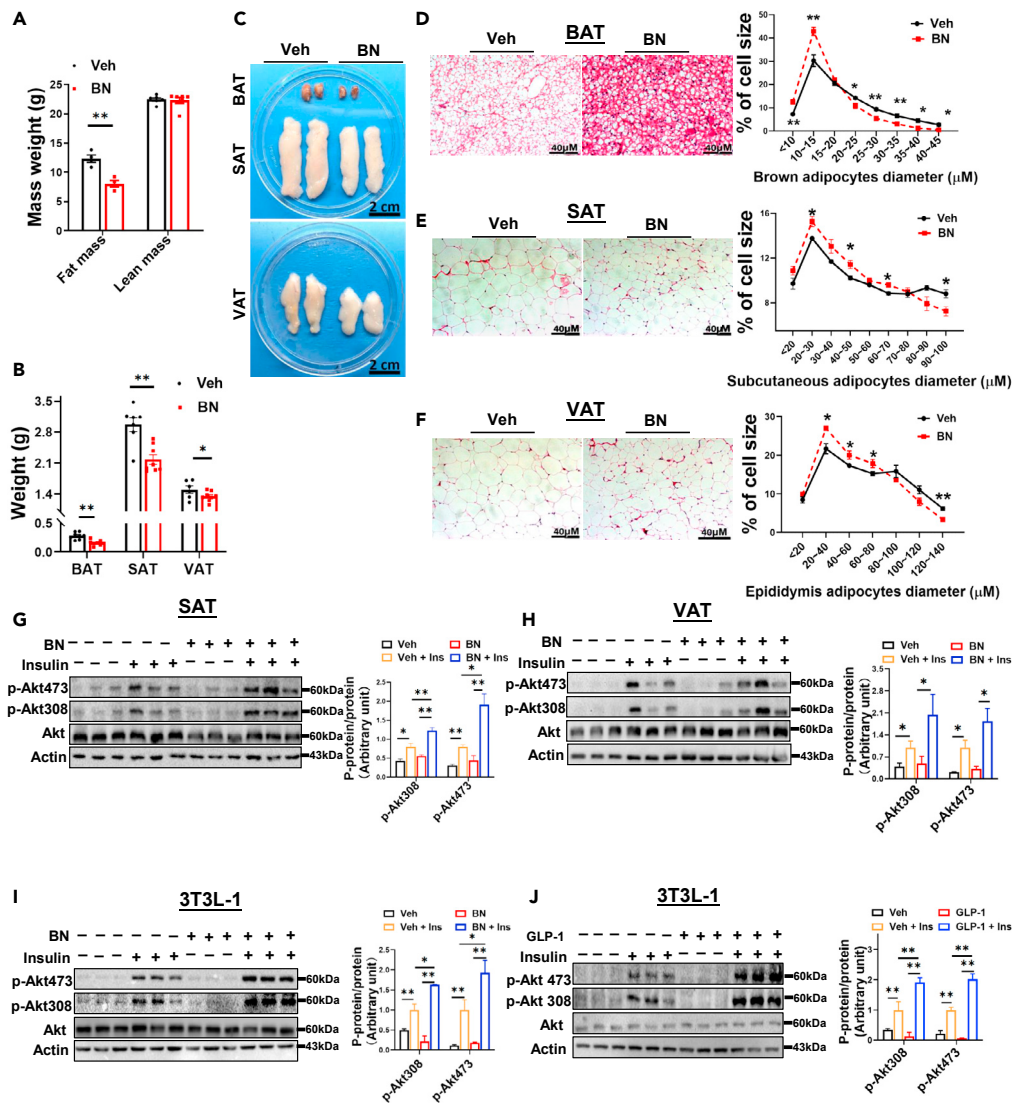


**Figure 2. Beinaglutide treatment decreases adipose tissue weight and adipocyte size and potentiates insulin sensitivity of adipocytes in vivo and in vitro**

(A) Body composition, (B) tissue weight, and (C) representative images of adipose tissues of obese mice after 6-week BN or Veh treatment ( $n = 8/\text{group}$ ). Representative images of hematoxylin and eosin staining of tissue sections (left panel) and measurements of adipocyte sizes (right panel) of BAT (D), SAT (E), and VAT (F) from 6-week BN- or Veh-treated obese mice. Insulin signaling in the SAT (G) and VAT (H) of obese mice was determined by western blot ( $n = 3/\text{group}$ ). 3T3L-1 cells were cultured and treated with BN (I) or GLP-1 (J) along with or without insulin, and insulin signaling was determined by western blot ( $n = 3/\text{group}$ ).

Data are represented as mean  $\pm$  SEM. \* $p < 0.05$ , \*\* $p < 0.01$  versus vehicle control. BAT, brown adipose tissue; SAT, subcutaneous adipose tissue; VAT, visceral adipose tissue.

treatment in the adipose tissues (Figures 3A–3C). Based on the OPLS-DA model with variable importance of projection (VIP)  $> 1.0$  and  $p < 0.05$ , SAT displayed the most apparent changes, followed by BAT and VAT. About 312, 140, and 92 lipids in the SAT, BAT, and VAT, respectively, were differentiated between the two groups. Changes of the overall lipid composition and distribution in the three adipose tissues were shown in Figures 3A–3C. Figures 3D–3F showed top 10 pathway enrichments by Kyoto Encyclopedia of Genes and Genomes (KEGG) analyses, among of which glycerophospholipid (GP) metabolism pathway was listed in all three fat depots (Figures 3D–3F). Besides, insulin resistance, cholesterol metabolism, and adipocytokine signaling pathway were the common top enrichments in both BAT and SAT (Figures 3D and 3E).

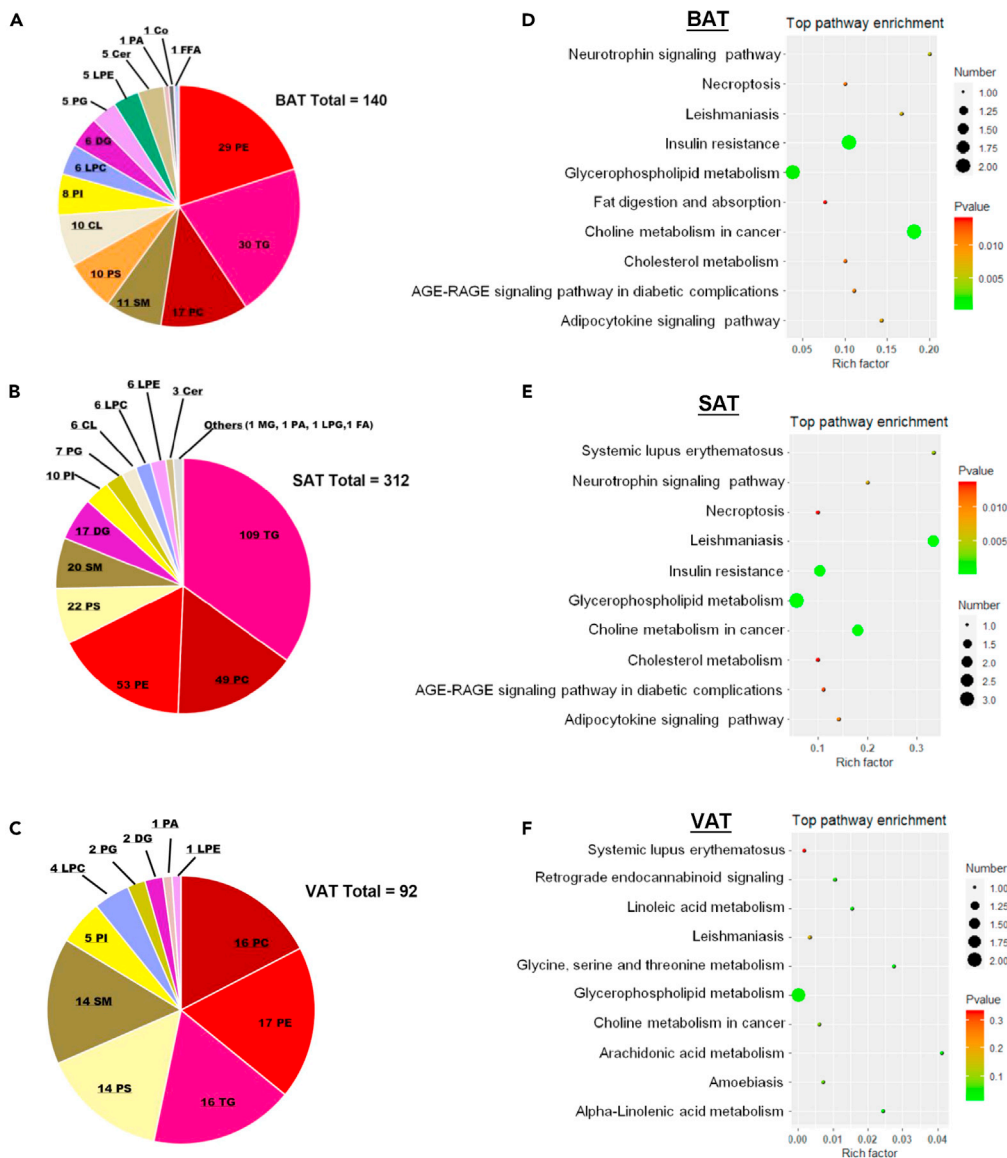


**Figure 3. Beinaglutide treatment alters lipidomic profiles of adipose tissues**

Eight-week-old C57BL/6 mice were fed with an HFD to induce obesity and then treated with Beinaglutide (BN) or vehicle (Veh) control through subcutaneous injection for 6 weeks. Lipids were extracted, and lipidomic analysis of adipose tissues was performed by LC-MS/MS. Distribution of lipid classes that were differentiated between the two groups in BAT (A), SAT (B), and VAT (C) were detected.

(D–F) Functional enrichment analyses using Kyoto Encyclopedia of Genes and Genomes (KEGG) pathways. The dot size indicates lipid numbers and color indicates corresponding significance values displayed as  $\log_{10}$  (p value).

BAT, brown adipose tissue; SAT, subcutaneous adipose tissue; VAT, visceral adipose tissue.

### Beinaglutide treatment alters glycerolipid components of adipose tissues

Glycerolipids (GLs), including TG, DG, and FFA, are the main components of adipose tissue and major substrates for lipid oxidation. There were no significant changes in the total abundance of TG and DG in the BAT (Figure 4A) and the VAT (Figure S4A), but there was a significant decrease in total abundance of DG in the SAT of treated mice (Figure 4B). Further analyses of the BAT showed 6 DG species that displayed significant changes and 5 of which showed reduced (Figure 4C). Sixteen changed DG species were detected, and 15 of them were significantly reduced in the SAT that was treated with BN when compared with those in the control mice (Figure 4D).

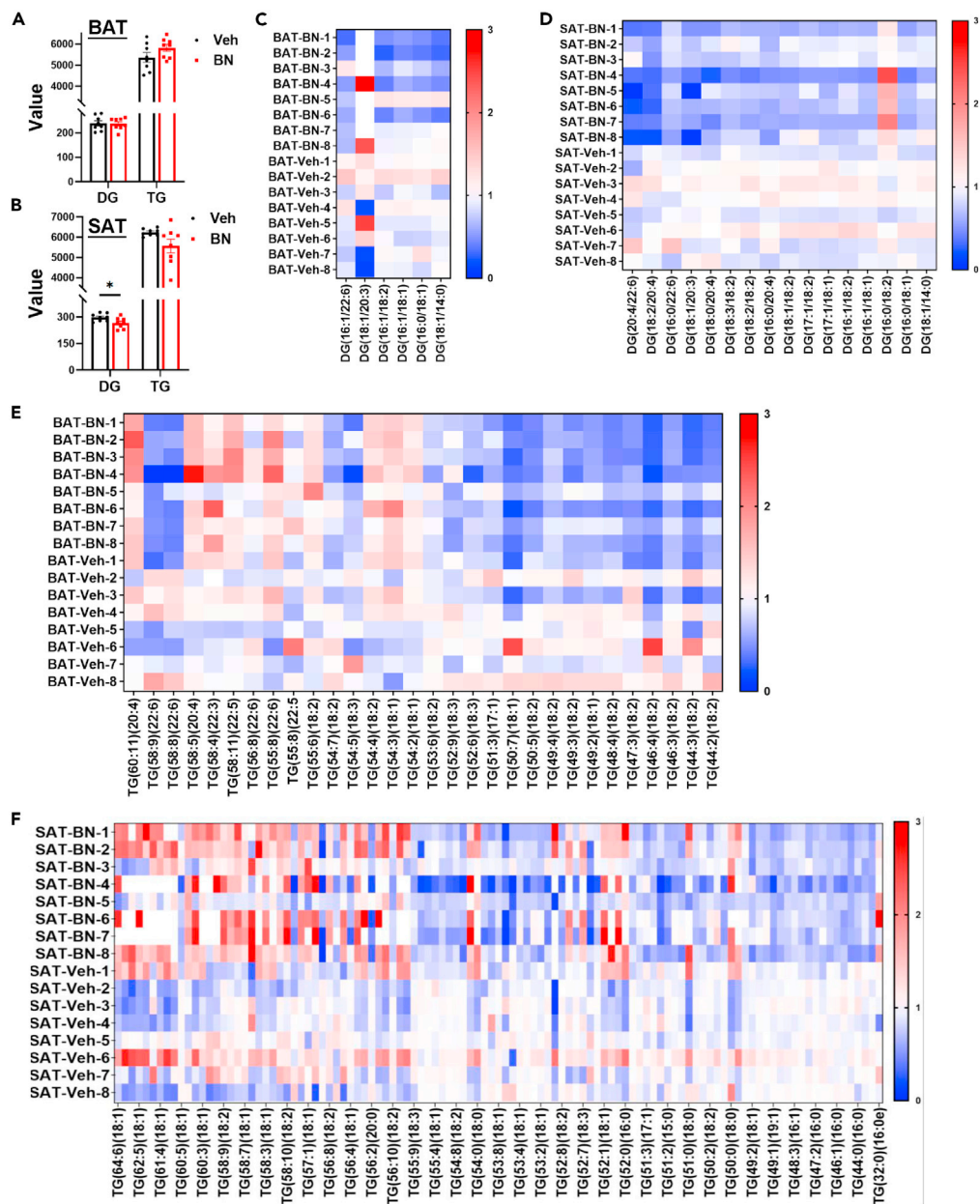


**Figure 4. Beinauglutide alters glycerolipid metabolism of adipose tissues**

Lipidomic analysis of adipose tissues was performed by LC-MS/MS in the HFD-induced obese mice treated with Beinauglutide (BN) or vehicle (Veh) control. Changes of overall abundance of triglycerides (TG) and diglyceride (DG) in the BAT (A) and SAT (B) were detected ( $n = 8/\text{group}$ ). Heatmap analyses show DG species in the BAT (C) and the SAT (D) and TG species in the BAT (E) and the SAT (F).

Data were presented as mean  $\pm$  SEM. \* $p < 0.05$  versus control. BAT, brown adipose tissue; SAT, subcutaneous adipose tissue.

Numerous altered TG species were observed, including 30 in the BAT and 109 in the SAT, respectively (Figures 4E and 4F). However, quite fewer altered DG and TG species were observed in the VAT (Figures S4B and S4C). In the demand of energy, TGs with very long chain fatty acids in lipid droplets can be mobilized and transported rapidly to peroxisomes for fatty acid oxidation. After BN treatment, in the BAT and SAT, the most upregulated TG species were chain lengths of 55 carbons or more ( $C \geq 55$ ), whereas chain lengths of 54 carbons or less ( $C \leq 54$ ) were the most downregulated (Figures 4E and 4F). However, in the BAT, the fractions that were significantly induced were TGs of major abundance, including C54:2, C54:3, and C54:4,

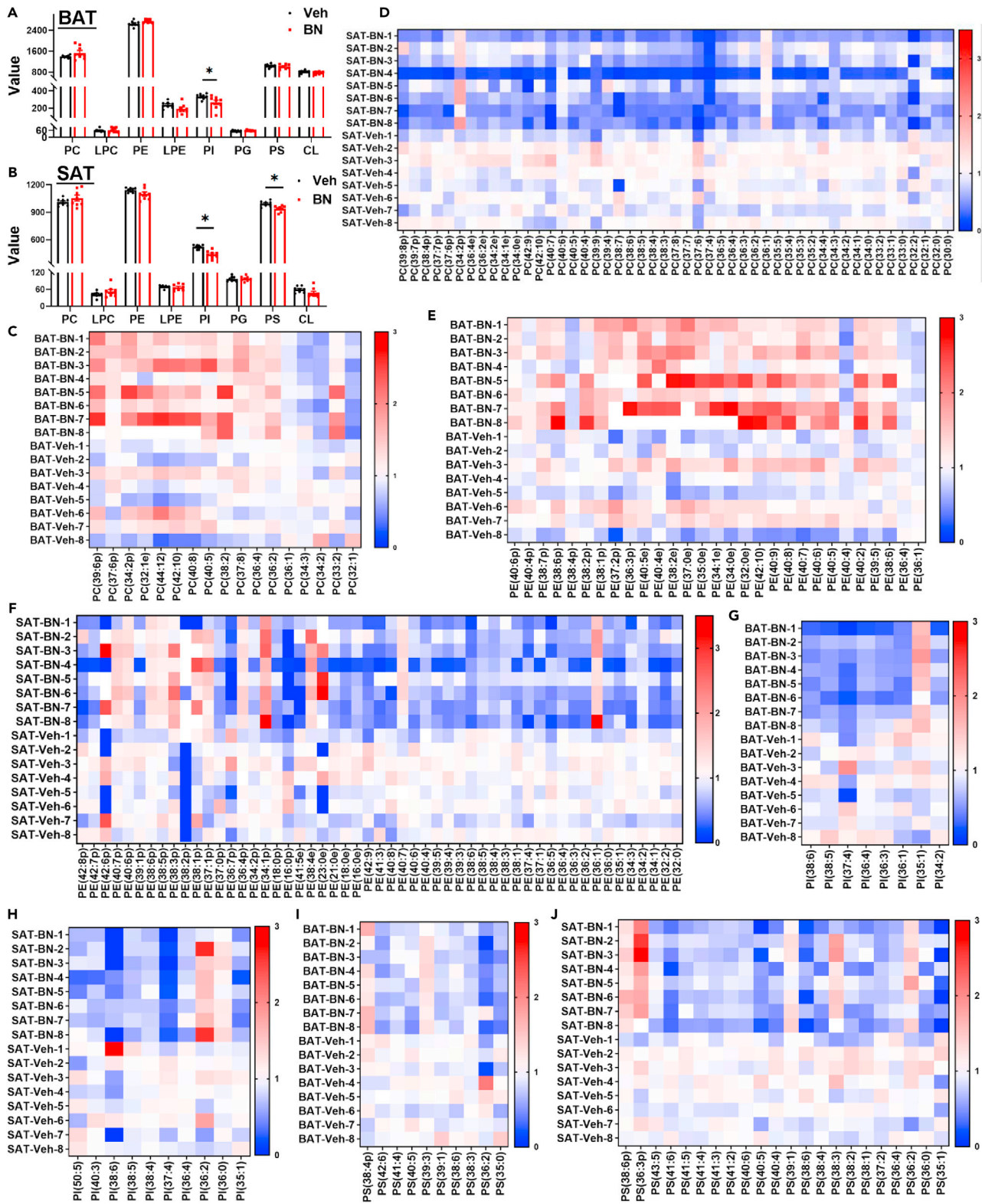


**Figure 5. Beinaglutide alters glycerophospholipid metabolism of adipose tissues**

Lipidomic analysis of adipose tissues was performed by LC-MS/MS in the HFD-induced obese mice treated with Beinaglutide (BN) or vehicle (Veh) control. Changes of overall abundance of major glycerophospholipids in the BAT (A) and SAT (B) were detected ( $n = 8/\text{group}$ ). Heatmap analyses show phosphatidylcholine (PC) species in the BAT (C) and the SAT (D), phosphatidylethanolamines (PE) species in the BAT (E) and the SAT (F), phosphatidylinositol (PI) species in the BAT (G) and the SAT (H), and phosphatidylserine (PS) species in the BAT (I) and the SAT (J). Data were presented as mean  $\pm$  SEM. \* $p < 0.05$  versus control. BAT, brown adipose tissue; SAT, subcutaneous adipose tissue.

whereas the most induced TGs were middle (C56:8, C58:2, C58:3, C58:7, C58:8) and minor (C54:0, C54:1, C56:1, C56:2) abundant species in the SAT.

**Beinaglutide treatment alters glycerophospholipid metabolism of adipose tissues**

Glycerophospholipids (GPs) are major components of cellular membranes and also regulate membrane fluidity, dynamics, and homeostasis (Hishikawa et al., 2014). We found that the overall abundance of the GP subclasses, including PC, PE, cardiolipin (CL), lysophosphatidylcholine (LPC), and lysophosphatidylethanolamine (LPE) was comparable between the groups (Figures 5A, 5B, and S5A), except the levels of phosphatidylinositol (PI) in the three adipose depots (Figures 5A, 5B, and S5A), and phosphatidylserine (PS) in the SAT (Figure 5B) and VAT (Figure S5A) decreased significantly in the treated mice. Next, we analyzed whether the composition of the major GP subclasses including PC, PE, PI, and PS was affected by the BN treatment. Interestingly, there were numerous altered PC species and most of them increased in the BAT (Figure 5C) and SAT (Figure 5D), whereas in the VAT we observed a decline pattern (Figure S5B).

The LC-MS analyses showed that BAT contains higher level of PE than SAT and VAT, and most PE species that were altered increased in the BAT (Figure 5E) but decreased in the SAT (Figure 5F) and VAT (Figure S5C), indicating the different responses of PE in the BAT and WAT to the BN treatment. PI species containing C36 and C38 are the major species. We found that overall PI levels and C36 and C38 species decreased in all three adipose tissues (Figures 5G, 5H, and S5D). PS is the major source of regulating molecular in lipid synthesis and lipid transportation. We found that most of the altered PS species in the three adipose tissues decreased (Figures 5I, 5J, and S5E). As abnormal contents of GPs and subclasses could contribute to dyslipidemia, obesity, and insulin resistance (Merino et al., 2018; Raubenheimer et al., 2006; Razquin et al., 2018), our studies indicate that BN treatment might have beneficial effects on adipose tissues through the regulation of lipid composition and facilitation of lipolysis.

**Beinaglutide treatment alters sphingolipid metabolism of adipose tissues**

Although much less abundant than GLs and GPs in the adipocytes, sphingolipids (SLs), typically representing 2%–15% of the total cellular lipidome, are essential cellular lipids that function as structural membrane components. Ceramide (Cer), the simplest class of SLs, is responsible for regulating a broad range of cellular signaling including pro-inflammatory cytokine activation. Recent studies have revealed that overnutrition can cause accumulation of Cer, which can lead to insulin resistance, dyslipidemia, and ultimately cell death that is associated with many metabolic disorders (Chaurasia and Summers, 2021). We observed that the overall Cer levels in the BAT and SAT decreased (Figures 6A–6C) but were comparable in the VAT (Figure S6A) of BN-treated mice. Further analysis of the Cer profiles revealed that majority of the decreased fractions were Cer d18:1 with acyl chains from C16 to C24 in both BAT and SAT (Figures 6B–6D). Previous studies have reported that adipose Cer synthesis can be suppressed by cold or  $\beta$ -adrenergic agonists, and inhibition of Cer promotes adipose browning, thus alleviating obesity-associated inflammation, and improves whole body metabolism (Chaurasia et al., 2016). The decreased Cer levels in our results suggest that BN treatment might induce adipose tissue browning and thermogenesis by inhibiting Cer synthesis or promoting degradation.

Interestingly, the overall sphingomyelin (SM) levels and several species of SM with higher acyl-chain carbon numbers (>33 carbons) in the SAT (Figures 6C and 6E) and VAT (Figures S6A and S6B) were induced significantly in the BN-treated mice. The increased SM was also observed in the SAT of short-term cold temperature (4°C) exposure (Xu et al., 2019). Taken together, our data indicate that BN treatment might promote adipose tissue browning and thermogenesis by inhibiting Cer synthesis and inducing SM levels in the adipose tissues.

**Beinaglutide changes the expression of genes involved in lipid metabolism and thermogenesis in the SAT**

To determine whether rhGLP-1 BN altered the transcriptional profiles of adipose tissues, we performed RNA-seq analysis using the RNAs isolated from the same tissue samples of lipidomics. As our lipidomic

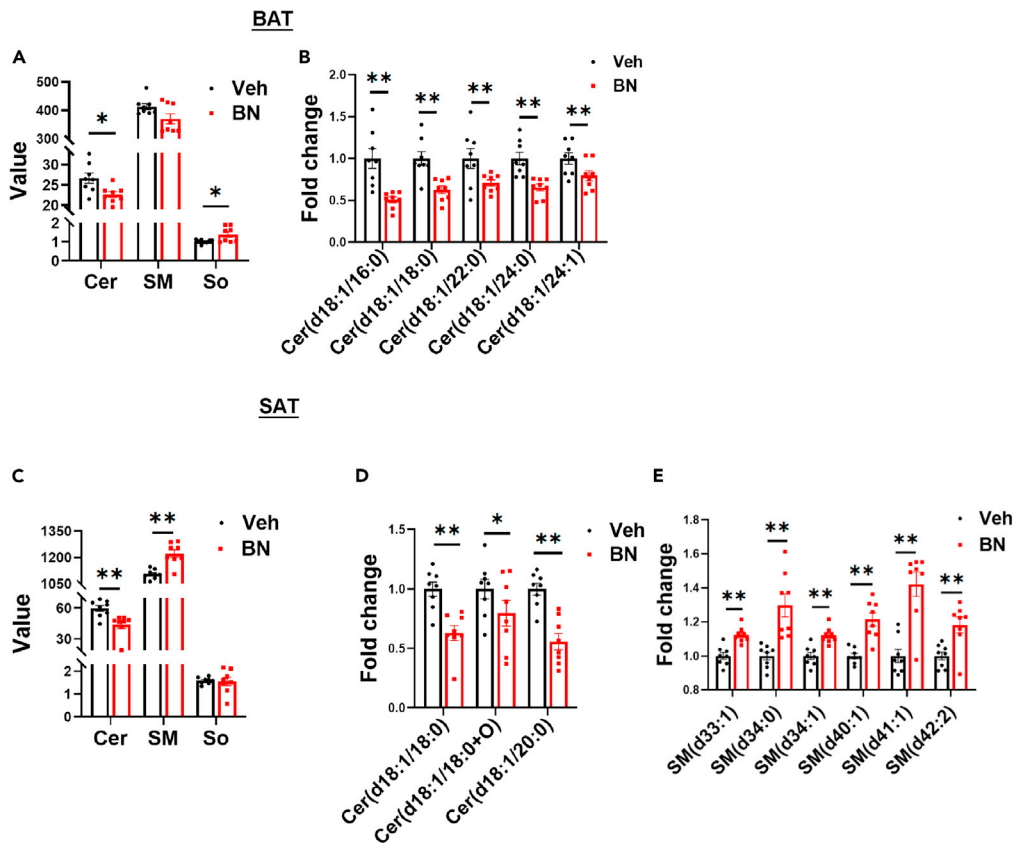


**Figure 6. Beinaglutide alters sphingolipid metabolism of adipose tissues**

Lipidomic analysis of adipose tissues was performed by LC-MS/MS in the HFD-induced obese mice treated with Beinaglutide (BN) or vehicle (Veh) control. Changes of overall abundance of major sphingolipid in the BAT (A) and SAT (C) were detected (n = 8/group). Change of Ceramide (Cer) species were detected in the BAT (B) and the SAT (D).

(E) Changes of sphingomyelin (SM) species in the SAT were showed.

Data are represented as mean  $\pm$  SEM. \*p < 0.05; \*\*p < 0.01 versus control. BAT, brown adipose tissue; SAT, subcutaneous adipose tissue.

data have shown that, in response to the BN administration, the most dramatic changes of lipid profile happened in the SAT, we next focused on this fat depot for the transcriptomic profiling. A total of 1,286 genes were detected to have changed dramatically in BN and control groups using a significance level of false discovery rate (FDR) < 0.05. Among of them, 832 genes were downregulated, whereas 454 were upregulated (Figure 7A).

The KEGG analyses revealed that insulin-signaling-related PI3K-AKT pathway, PPAR signaling, and several lipid-metabolism-related pathways, including GL metabolism and cholesterol metabolism (Figure 7B), are among the top enriched pathways in the SAT.

We then analyzed the genes that were significantly altered for important enzymes or regulators and their involved pathways of GLs, GPs, and SLs. As shown in Figure 7C, the major genes involved in lipogenesis decreased in the BN-treated SAT, including ATP citrate lyase (gene *Acly*), an important enzyme-linking carbohydrate for lipid metabolism by generating acetyl-CoA from citrate for fatty acid and cholesterol biosynthesis; acetyl-coenzyme A carboxylase 1 (gene *Acaa1*), a biotin-containing enzyme that catalyzes the carboxylation of acetyl-CoA to malonyl-CoA for fatty acid synthesis; and fatty acid synthase (gene *Fasn*), an enzyme catalyzing synthesis of palmitate from acetyl-CoA and malonyl-CoA into long-chain saturated fatty acids. In contrast, genes that were crucial for lipolysis were upregulated (Figure 7C), including hormone-sensitive lipase (HSL, gene *Lipe*) and patatin-like phospholipase domain containing 2 (PNPLA2, gene *Pnpla2*)/adipocyte triglyceride lipase (ATGL), both of which are rate-limiting enzymes of the lipolysis catalyzing the release of fatty acids from storage TG in adipocytes (Fruhbeck et al., 2014; Yang and Mottillo,

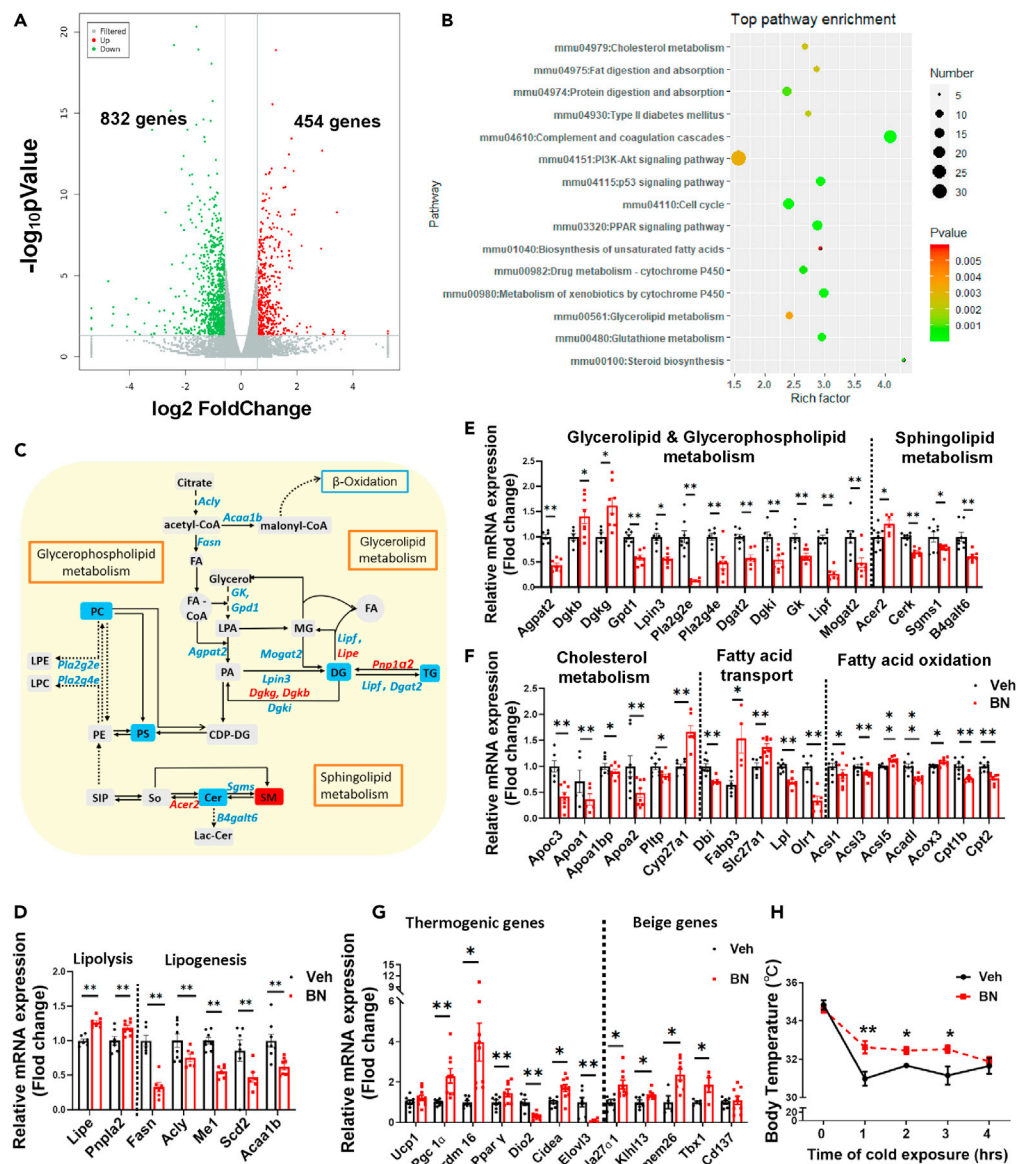


**Figure 7. Beinaglutide changes the expression of genes involved in lipid metabolism and thermogenesis in the subcutaneous adipose tissue**

Eight-week-old C57BL/6 mice were fed with an HFD to induce obesity and then treated with Beinaglutide (BN) or vehicle (Veh) control through subcutaneous injection for 6 weeks. (A) Log<sub>2</sub> fold changes in exons of RNA-Seq gene bodies in the SAT of BN-treated versus control mice and the corresponding significance values displayed as log<sub>10</sub> (p value). The transverse and vertical gray lines indicate the cutoff value for differential expression (FDR < 0.05 & Abs (Log<sub>2</sub> fold changes) > 0.5). In total, 454 and 832 genes were identified that had induced (red) or repressed (green) expression levels by BN administration in the SAT.

(B) Functional enrichment analyses using Kyoto Encyclopedia of Genes and Genomes (KEGG) pathways. The dot size indicates gene numbers and color indicates corresponding significance values displayed as log<sub>10</sub> (p value).

(C) Selected glycerolipid and glycerophospholipid metabolic reactions from KEGG, with indications of quantified lipid classes and genes (encoding proteins that catalyze the indicated conversions) significantly regulated in the SAT by BN treatment. Blue and red colors indicate decreased and increased total concentration of the lipid classes or expression of the genes, respectively.

(D) Relative expression levels of selected genes involved in lipolysis and lipogenesis from the RNA-seq dataset for BN-treated and control mice.

(E) Relative expression levels of selected genes from the RNA-seq dataset for important enzymes or regulators that involve in metabolism of glycerolipids, phospholipids, and sphingolipids.

**Figure 7. Continued**

(F) Relative expression levels of selected genes involved in cholesterol metabolism, fatty acid transport, and beta oxidation.

(G) Relative expression levels of genes involved in thermogenesis and beiging in the SAT.

(H) The responses of obese mice to cold temperature. Obese mice maintained in single cage treated with BN or vehicle were kept at room temperature (25°C) or cold chamber (6°C) for 4 h.

Data are represented as mean  $\pm$  SEM. The rectal temperature was measured by a temperature sensor (n = 8/group).

\*p < 0.05; \*\*p < 0.01 versus control.

2020). The genes diacylglycerol kinase gamma (*Dgkg*) and diacylglycerol kinase Beta (*Dgkb*) are family members of diacylglycerol kinases (DGKs) that attenuate DG signaling by converting this lipid to phosphatidic acid (PA) (Topham, 2006). Both genes were upregulated by BN treatment (Figure 7C). The increased expression of these genes involved in DG and TG metabolism might contribute partly to the overall decrease in DG levels and specific species in the SAT (Figures 4B and 4D).

Alkaline ceramidase 2 (*Acer2*) is one of the ceramidases that plays key roles in the degradation of Cer into sphingosine and free fatty acids (Parveen et al., 2019). We found that expression level of *Acer2* increased dramatically (Figure 7C), which might partly account for the reduced Cer level in the SAT- of BN-treated mice (Figures 6C and 6D).

The RNA-seq detected genes that involve in rate-limiting steps of lipogenesis and lipolysis and metabolic pathways of GLs, GPs, SLs, and cholesterol as well as fatty acid transport/oxidation are shown in Figures 7D–7F and also verified by real-time RT-PCR (data not shown). The aforementioned findings demonstrate that the composition of fatty-acyl chains associated with major lipids changed markedly upon BN administration, which could be a result of increased or decreased expression of genes encoding enzymes involved in lipolysis or lipogenesis, respectively.

Because previous studies have reported GLP-1 and analogs have promoting effects on thermogenesis (Fang et al., 2021; Zhang et al., 2019), we determined whether BN has similar actions on the obese mice. The basal metabolic rate (BMR), as determined by oxygen consumption (VO<sub>2</sub>) (Figure S7A) and respiration exchange ratio (RER) (Figure S7B) using Oxymax/CLAMS metabolic cages, was not significantly different between the two groups. BN treatment caused the expression of some thermogenic genes to increase, including *Prdm16*, *Pgc1α*, *Pparγ*, and *Cidea*, as well as beige marker genes, including *Tmem26*, *Tbx1*, *Klh13*, and *Scla27*, in the SAT of the obese mice, except *Dio2* and *Elvol3* (Figure 7G), suggesting beige fat promoting effects of the BN. The protein levels of thermogenic genes (PRDM16, UCP1) also increased in the BAT of BN-treated mice (Figure S7C).

To further determine whether BN administration had any effects on the thermogenesis, we put the BN-treated and control mice in cold temperature (6°C) for 4 h. In response to acute cold stress, BN-treated obese mice showed slower decrease of body temperature compared with the controls (Figure 7H), implying enhanced cold tolerance of these mice.

## DISCUSSION

As a recombinant human GLP-1, BN shares 100% homology with human GLP-1(7–36). Our unpublished data have shown that BN stimulates GLP-1R-dependent cAMP formation in the HEK 293 cell and enhances glucose-stimulated insulin release (GSIS) in mouse islets, implying that BN may have the same biological activities as GLP-1, which are also supported by our published studies (Fang et al., 2021; Tao et al., 2019; Zhang et al., 2019). The pharmacokinetic profiles in C57BL/6 mice have revealed that the T<sub>max</sub> of BN is about 5 min (Fang et al., 2021), which is similar to that of the endogenous GLP-1, as its half-life in plasma is about 1.5–5 min. Based on this information, we consider BN to be a short-acting GLP-1. The clinical and laboratory research data show that BN is not only effective for T2DM but also has benefits on weight loss and NASH treatment. Our study confirmed that BN-treated obese mice had significantly reduced food intake, body weight, adiposity, and fatty liver. These effects were similar to many GLP-1 analogs, such as liraglutide and semaglutide (Beiroa et al., 2014; Gabery et al., 2020; Lopez et al., 2015). GLP-1 and its analogs are well known to extend the phase of gastric emptying and reduce food intake largely through humoral pathways involving direct action on brain GLP-1R that is widely expressed in various hypothalamic nuclei, hindbrain nuclei, hippocampus, and nuclei embedded within the mesolimbic reward circuitry (Kanoski et al., 2016; Ronveaux et al., 2015). We previously reported that BN can retard gastric

emptying and reduce food intake (Fang et al., 2021), similar to other short-acting GLP-1 analogs. Although we are unable to provide direct evidence in this study, we can hypothesize that BN could regulate food intake through activating GLP-1R-related signaling in the central nervous system (CNS), which deserves further investigation in the future.

Previous studies have shown that the weight loss effect of GLP-1 analogs is mainly caused by decreased food intake and/or the activation of BAT thermogenesis through GLP-1R-dependent signaling pathway in the CNS (Beiroa et al., 2014; Fortin et al., 2020). Central administration of liraglutide increases the sympathetic output to BAT, boosts BAT thermogenesis, and promotes WAT browning in mice, and its effects are mediated by the activation of GLP-1R in the hypothalamic ventromedial nucleus (VMH) (Beiroa et al., 2014; Lopez et al., 2015) or the dorsomedial hypothalamus (DMH) (Lee et al., 2018). We observed induced expression of thermogenic and beige gene in the SAT and BAT as well as enhanced cold tolerance. As the increased BMR of the obese mice was not observed in BN-treated mice, we speculate that the physiological observations on body weight, adipose tissue, and glucose tolerance/insulin response might be mainly caused by suppressed food intake and decreased lipid metabolism in the liver; however, increased BAT activity and SAT beigeing effects might also play a role.

Interestingly, we observed that plasma levels of insulin decreased significantly after 6-week BN administration. As a potent incretin hormone, GLP-1 is known for stimulating insulin secretion. Our recent work has shown that BN administration improved insulin secretion in ob/ob mice greatly, with about 5-fold increase 30 min after peptide injection and about 33.5-fold increase 15 min after glucose loading (Fang et al., 2021). The 2-week administration of liraglutide has a tendency to reduce blood insulin levels in diet-induced obese mice (Buganova et al., 2017). In our study, we collected plasma and measured insulin levels after over-night fasting, which had been about 18 h after final injection, when the insulin-promoting effects of BN might have diminished. A large board of studies and clinical correlations has suggested that hyperinsulinemia is associated with obesity, and there is a close relationship between hyperinsulinemia and dyslipidemia (Corkey, 2011; Erion and Corkey, 2017). However, recent *in vivo* evidence has also shown that reducing circulating insulin levels may protect and reverse adiposity, insulin resistance, and hyperglycemia that is associated with obesity (Page and Johnson, 2018).

Consistent to what was observed in liraglutide- (Buganova et al., 2017; Decara et al., 2018) or Exendin-4 (Wei et al., 2015) injected obese mice, BN treatment significantly decreased plasma leptin levels. Our results suggest that 6-week BN treatment could reduce hyperinsulinemia and hyperleptinemia associated with obesity.

Adipose tissues are important regulators of whole-body energy homeostasis. In this study, we focused on the actions of rhGLP-1 BN on adipose metabolism and found that BN has several beneficial effects on the adipose tissues of obese mice. First, cell size and turnover of adipocytes are major determinants of fat tissue metabolism and mass, the alterations of which are associated with pathological conditions (Morigny et al., 2021). BN-treated mice not only show dramatically reduced adipose tissue weight but also have more small adipocytes, but fewer large adipocytes. Hypertrophy (an increase in cell size) of adipocyte is closely associated with dyslipidemia and insulin resistance in humans (Hoffstedt et al., 2010; Veilleux et al., 2011). A reduction in adipocyte size induced by BN may indicate improvement of insulin sensitivity in the fat tissues of obese mice.

Second, it is well established that GLP-1 analogs improve insulin sensitivity in animals and humans. However, current available evidence seems to suggest that, independent of stimulation of insulin and inhibition of glucagon secretion, whether GLP-1 has direct or indirect effects on insulin signaling or glucose uptake in peripheral tissues is still controversial (Drucker, 2018). In our study, we discovered that although its application alone has no effects, BN can enhance insulin-stimulated phosphorylation of AKT when cells were co-cultured with BN and insulin, implying that BN can potentiate insulin signaling of WAT, particularly in the SAT. The same effects were observed in cultured 3T3-L1 cells and were also confirmed in GLP-1-treated 3T3-L1 cells. Subcutaneous administration of liraglutide decreased expression of genes/proteins involved in lipogenesis, peroxisomal  $\beta$ -oxidation, and lipid flux/storage (Decara et al., 2016), which may be partly due to the co-operative action of GLP-1R and  $\beta$ 3-adrenergic receptors in rat adipose tissues (Decara et al., 2018). *In vitro* studies have shown that liraglutide or GLP-1 could stimulate preadipocytes differentiation and lipid accumulation through different signaling pathways, such as MAPK, AKT, Wnt- $\beta$  catenin,

etc. We observed low but stably expressed GLP-1R gene and protein in the adipocytes (data not shown). However, whether BN acts on the cells through binding with GLP-1R and stimulating its associated signaling pathway alone or has an interaction with insulin signaling to argue the activity of insulin is still unknown and deserves further investigation.

Third, lipids are essential metabolites that have many crucial cellular functions, serving as the major structural and regulatory components of membranes, energy storage molecules, and inter- and intracellular signaling molecules (Han, 2016). They can provide a direct readout of cellular metabolic status. A comprehensive lipidomic evaluation that defines disease-specific lipid alterations with sufficient resolution to render identification of pathway perturbations, however, is still largely lacking for obese adipose tissues. In this study, we applied mass-spectrometry-based lipidomics and RNA-seq to extend our understanding of the alteration of lipids and their pathways in adipose tissues of obese mice. Our results have shown that BN induced significant declines in the overall levels of several lipid classes, including DG, PI, PS, and Cer, in the adipose tissues.

Although it is the simplest class of SLs, Cer play a key role in SL metabolism and serve both as the precursors and the breakdown products of other more complex SLs. There are at least two Cer biosynthesis pathways, the *de novo* synthesis and the hydrolysis from other SLs, e.g. sphingomyelin, glycosylceramide. In addition, Cer can be deacylated and degraded by ceramidases that break Cer into free fatty acid and sphingosine. Therefore, the metabolism of SL is an array of interconnected networks that are involved in many lipids and enzymes. Due to the limitations of our assay, we could not detect all classes of SLs and could not know the levels of other SLs. In the future, investigation of other SLs might help to explain the increased sphingomyelins and reduced level of Cer and expression of *Sgms1* in our study.

The lipidome profile of adipocytes can not only be directly remodeled by changes in dietary composition and quantity but also can be modified by negative energy balance conditions that influence lipid turnover and enzymatic machinery activity, such as thermal stress, physical activity, fasting, and cachexia (Francis et al., 2017; Grzybek et al., 2019; Marcher et al., 2015). Lipid species trigger specific signaling pathways to modulate cell function.

Our lipidomic profiles showed different adipose tissues' response to BN treatment. The TG, PE, and PC were the most abundant lipid classes altered by BN treatment in all three adipose tissues. However, SAT displayed much more altered numbers of lipid species than BAT and VAT. In line with the lipidomics, the transcriptomic profiling also revealed that the most dramatic changes of gene expression happened in the SAT, followed by BAT and VAT (data not shown). In addition, SAT also showed the most reduction in tissue weight. Taken together, the results suggest that different adipose tissues have different responses to the BN administration, with SAT having the most prominent alterations. SAT is the natural reservoir for excess energy. However, when this storage area becomes overwhelmed or its ability of expansion is impaired, excessive lipids will accumulate in other locations, including visceral depots and organs such as the liver and pancreas. Alterations of lipidomic and transcriptomic profiles in SAT may reflect the improved function of this fat depot after BN treatment.

It is well known that adipose tissues are morphologically and physiologically different. Due to their highly plastic characteristics, adipocytes can undergo transformations and change their function and metabolism depending on physiological or pathophysiological conditions, such as nutrients, cold temperature, and drug administration. Although the mechanism underlying adipose tissues' different responses to BN is still unclear, we have proposed that different adipose tissues, regulated either by different intercellular signaling pathways or by a distinct neuro-adipose axis, may perform a profound remodeling process in function as a response to BN treatment, which in turn partially alleviates obesity-associated fatty liver and impairment of lipid metabolism and improves insulin sensitivity.

It is well established that GLP-1/GLP-1R functions through activation of down-stream PKA-, MAPK-, or AMPK-related signaling pathways in various cells. We did not observe altered mRNA levels of GLP-1R in adipose tissues in our RNA sequencing data, which was also confirmed by real-time PCR and western blot analyses (data not shown). These results suggest that the effects of BN on adipose tissues might not be through its regulation on expression of GLP-1R. Previous studies have found that GLP-1R agonists improve adipose tissues functions of obese mice through CNS (Lee et al., 2018; Fortin et al., 2020) or iNKT

cells in adipose tissue (Lynch et al., 2016). Our unpublished data have shown that BN stimulates GLP-1R-dependent cAMP formation in HEK 293 cell, indicating that BN can activate cAMP-associated signaling. The KEGG analyses of the transcriptomic data have also shown that PI3K-AKT and PPAR signaling pathways and several lipid-metabolism-related pathways are among the top enriched pathways in the SAT. These results suggest that BN may regulate multiple signaling pathways in adipose tissues, which deserve further investigation.

Similar to those in liver and immune cells, alterations in calcium signaling also play a role in adipose tissue dysfunction in obesity and other metabolic diseases (Arruda and Hotamisligil, 2015). GLP-1 and its analogs have been reported to regulate intracellular calcium homeostasis in many cells, including cardiomyocytes (Hu et al., 2017; Huang et al., 2016), pancreatic beta cells (Leech et al., 1996), endothelial cells (Krasner et al., 2014), etc. However, there currently is no evidence showing GLP-1 regulated calcium homeostasis in different adipocytes.

Indeed, to fully understand the function of GLP-1 and its analogs in adipose tissues, it is necessary to explore the roles of these signaling pathways and intracellular calcium in GLP-1-treated adipocytes. The related information will provide further insight into potential mechanisms for the differential effects of GLP-1 on the different types of adipose tissues.

To summarize, this study shows that rhGLP-1 BN reduces HFD-induced body weight gain and fat accumulation in the adipose tissues and the liver and improves obesity-associated damages of serum lipid and hormone profiles. In addition, BN treatment increases insulin sensitivity of adipocyte *in vivo* and *in vitro*. Furthermore, BN treatment leads to marked changes in the composition of lipids and the expression of genes involved in lipid metabolism in the subcutaneous adipose tissues. Our results suggest important roles of rhGLP-1 BN on lipid metabolism and insulin activity in adipose tissues, and BN could alleviate obesity-associated fatty liver and dyslipidemia by improving the function of adipose tissues.

### Limitations of the study

We proposed that, as a recombinant human GLP-1 sharing 100% homology with human GLP-1(7–36), the rhGLP-1 BN may play similar important roles on the lipid metabolism and insulin activity in adipose tissues. At this point, at least two important questions remain to be elucidated. (1) We showed that BN treatment increases insulin signaling activity of the adipocytes *in vivo* and *in vitro*. However, the underlying mechanism is unclear. Studies using a ChIP-MS method are required to find the target of BN or GLP-1 in adipocytes. (2) BN treatment leads to marked changes in the composition of lipids and the expression of genes involved in lipid metabolism in the subcutaneous adipose tissues of obese mice. Whether these effects occur in human samples need to be verified in the future.

### STAR★METHODS

Detailed methods are provided in the online version of this paper and include the following:

- KEY RESOURCES TABLE
- RESOURCE AVAILABILITY
  - Lead contact
  - Materials availability
  - Data and code availability
- EXPERIMENTAL MODEL AND SUBJECT DETAILS
  - Animals
- METHOD DETAILS
  - Body composition, energy expenditure, and histological analysis
  - Cell culture and treatment
  - RNA sequencing and analyses
  - Western blotting
  - Plasma lipid and hormone measurements
  - Adipose tissue lipid extraction
  - Lipidomics analysis
- QUANTIFICATION AND STATISTICAL ANALYSIS

## SUPPLEMENTAL INFORMATION

Supplemental information can be found online at <https://doi.org/10.1016/j.isci.2021.103382>.

## ACKNOWLEDGMENTS

We thank Dr Guanghou Shui for the help of lipidomic analysis and Ms Xueyi Pan for language editing. We thank the Shanghai LuMing Biological Technology co., LTD (Shanghai, China) for providing RNA-seq services.

This work was supported by grants from National Key R&D Program, China (2020YFA0803604), National Natural Science Foundation, China (91957113& 31871180), and Natural Science Foundation of Hunan Province (2019JJ40410) to F.H. and National Nature Science Foundation of China (81820108007) to Z.Z.

## AUTHORS CONTRIBUTIONS

F.Z. collected and assembled data and prepared the first draft of the manuscript. Z.C., D.W., L.T., Q.C., Y.Y., W.C., X.W., P.W., Y.Q., and W.Y. collected data. Z.Z. contributed to project initiation and discussion. Z.D. supervised the work; contributed to design, data analysis, and discussion; and gave final approval of the manuscript. F.H. contributed to conceptualization and design, data analysis and interpretation, and manuscript writing; contributed to financial support; and gave final approval of the manuscript. All authors reviewed and approved the manuscript.

## DECLARATION OF INTERESTS

The authors declare no competing interests.

Received: June 21, 2021

Revised: September 19, 2021

Accepted: October 27, 2021

Published: December 17, 2021

## REFERENCES

- Adan, R.A. (2013). Mechanisms underlying current and future anti-obesity drugs. *Trends Neurosci.* 36, 133–140. <https://doi.org/10.1016/j.tins.2012.12.001>.
- Agersù, H., Jensen, L.B., Elbrùnd, B., Rolan, P., and Zdravkovic, M. (2002). The pharmacokinetics, pharmacodynamics, safety and tolerability of NN2211, a new long-acting GLP-1 derivative, in healthy men. *Diabetologia* 45, 195–202. <https://doi.org/10.1007/s00125-001-0719-z>.
- Al-Sulaiti, H., Diboun, I., Banu, S., Al-Emadi, M., Amani, P., Harvey, T.M., Dömling, A.S., Latiff, A., and Elrayess, M.A. (2018). Triglyceride profiling in adipose tissues from obese insulin sensitive, insulin resistant and type 2 diabetes mellitus individuals. *J. Transl. Med.* 16, 175. <https://doi.org/10.1186/s12967-018-1548-x>.
- Alber, A., Bronden, A., and Knop, F.K. (2017). Short-acting glucagon-like peptide-1 receptor agonists as add-on to insulin therapy in type 1 diabetes: a review. *Diabetes Obes. Metab.* 19, 915–925. <https://doi.org/10.1111/dom.12911>.
- Arruda, A.P., and Hotamisligil, G.S. (2015). Calcium homeostasis and organelle function in the pathogenesis of obesity and diabetes. *Cell Metab.* 22, 381–397. <https://doi.org/10.1016/j.cmet.2015.06.010>.
- Babenko, A.Y., Savitskaya, D.A., Kononova, Y.A., Trofimova, A.Y., Simanenkova, A.V., Vasilyeva, E.Y., and Shlyakhto, E.V. (2019). Predictors of effectiveness of glucagon-like peptide-1 receptor agonist therapy in patients with type 2 diabetes and obesity. *J. Diabetes Res.* 2019, 1365162. <https://doi.org/10.1155/2019/1365162>.
- Beiroa, D., Imbernon, M., Gallego, R., Senra, A., Herranz, D., Villaroya, F., Serrano, M., Fernø, J., Salvador, J., Escalada, J., et al. (2014). GLP-1 agonism stimulates Brown adipose tissue thermogenesis and browning through hypothalamic AMPK. *Diabetes* 63, 3346–3355. <https://doi.org/10.2337/db14-0302>.
- Blüher, M. (2019). Obesity: global epidemiology and pathogenesis. *Nat. Rev. Endocrinol.* 15, 288–298. <https://doi.org/10.1038/s41574-019-0176-8>.
- Buganova, M., Pelantova, H., Holubova, M., Sediva, B., Maletinska, L., Zelezna, B., Kunes, J., Kacer, P., Kuzma, M., and Haluzik, M. (2017). The effects of liraglutide in mice with diet-induced obesity studied by metabolomics. *J. Endocrinol.* 233, 93–104. <https://doi.org/10.1530/JOE-16-0478>.
- Caesar, R., Manieri, M., Kelder, T., Boekschoten, M., Evelo, C., Muller, M., Kooistra, T., Cinti, S., Kleemann, R., and Drevon, C.A. (2010). A combined transcriptomics and lipidomics analysis of subcutaneous, epididymal and mesenteric adipose tissue reveals marked functional differences. *PLoS One* 5, e11525. <https://doi.org/10.1371/journal.pone.0011525>.
- Chaurasia, B., and Summers, S.A. (2021). Ceramides in metabolism: key lipotoxic players. *Annu. Rev. Physiol.* 83, 303–330. <https://doi.org/10.1146/annurev-physiol-031620-093815>.
- Chaurasia, B., Kaddai, V.A., Lancaster, G.I., Henstridge, D.C., Sriram, S., Galam, D.L., Gopalan, V., Prakash, K.N., Velan, S.S., Bulchand, S., et al. (2016). Adipocyte ceramides regulate subcutaneous adipose browning, inflammation, and metabolism. *Cell Metab.* 24, 820–834. <https://doi.org/10.1016/j.cmet.2016.10.002>.
- Corkey, B.E. (2011). Banting lecture 2011: hyperinsulinemia: cause or consequence? *Diabetes* 61, 4–13.
- D'Alessio, D., Vahl, T., and Prigeon, R. (2004). Effects of glucagon-like peptide 1 on the hepatic glucose metabolism. *Horm. Metab. Res.* 36, 837–841. <https://doi.org/10.1055/s-2004-826172>.
- Danaei, G., Finucane, M.M., Lu, Y., Singh, G.M., Cowan, M.J., Paciorek, C.J., Lin, J.K., Farzadfar, F., Khang, Y.-H., Stevens, G.A., et al. (2011). National, regional, and global trends in fasting plasma glucose and diabetes prevalence since 1980: systematic analysis of health examination surveys and epidemiological studies with 370 country-years and 2.7 million participants. *Lancet* 378, 31–40. [https://doi.org/10.1016/S0140-6736\(11\)60679-X](https://doi.org/10.1016/S0140-6736(11)60679-X).
- Decara, J., Arrabal, S., Beiroa, D., Rivera, P., Vargas, A., Serrano, A., Pavon, F.J., Ballesteros, J., Rodriguezde, F., Fonseca, et al. (2016). Antiobesity efficacy of GLP-1 receptor agonist

- liraglutide is associated with peripheral tissue-specific modulation of lipid metabolic regulators. *Biofactors* 42, 600–611. <https://doi.org/10.1002/biof.1295>.
- Decara, J., Rivera, P., Arrabal, S., Vargas, A., Serrano, A., Pavon, F.J., Dieguez, C., Nogueiras, R., Rodriguez de Fonseca, F., and Suarez, J. (2018). Cooperative role of the glucagon-like peptide-1 receptor and beta3-adrenergic-mediated signalling on fat mass reduction through the downregulation of PKA/AKT/AMPK signalling in the adipose tissue and muscle of rats. *Acta Physiol.* 222. <https://doi.org/10.1111/apha.13008>, e130080–e130020.
- Doyle, M.E., and Egan, J.M. (2007). Mechanisms of action of glucagon-like peptide 1 in the pancreas. *Pharmacol. Ther.* 113, 546–593. <https://doi.org/10.1016/j.pharmthera.2006.11.007>.
- Drucker, D.J. (2018). Mechanisms of action and therapeutic application of glucagon-like peptide-1. *Cell Metab.* 27, 740–756. <https://doi.org/10.1016/j.cmet.2018.03.001>.
- Drucker, D.J., Buse, J.B., Taylor, K., Kendall, D.M., Trautmann, M., Zhuang, D., and Porter, L. (2008). Exenatide once weekly versus twice daily for the treatment of type 2 diabetes: a randomised, open-label, non-inferiority study. *Lancet* 372, 1240–1250. [https://doi.org/10.1016/S0140-6736\(08\)61206-4](https://doi.org/10.1016/S0140-6736(08)61206-4).
- Elvert, R., Herling, A.W., Bossart, M., Weiss, T., Zhang, B., Wenski, P., Wandschneider, J., Kleutsch, S., Butty, U., Kannt, A., et al. (2018). Running on mixed fuel-dual agonistic approach of GLP-1 and GCG receptors leads to beneficial impact on body weight and blood glucose control: a comparative study between mice and non-human primates. *Diabetes Obes. Metab.* 20, 1836–1851. <https://doi.org/10.1111/dom.13212>.
- Erion, K.A., and Corkey, B.E. (2017). Hyperinsulinemia: a cause of obesity? *Curr. Obes. Rep.* 6, 178–186. <https://doi.org/10.1007/s13679-017-0261-z>.
- Fang, X., Du, Z., Duan, C., Zhan, S., Wang, T., Zhu, M., Shi, J., Meng, J., Zhang, X., Yang, M., et al. (2021). Beinaglutide shows significantly beneficial effects in diabetes/obesity-induced nonalcoholic steatohepatitis in ob/ob mouse model. *Life Sci.* 270, 118966. <https://doi.org/10.1016/j.lfs.2020.118966>.
- Fortin, S.M., Lipsky, R.K., Lhamo, R., Chen, J., Kim, E., Borner, T., Schmidt, H.D., and Hayes, M.R. (2020). GABA neurons in the nucleus tractus solitarius express GLP-1 receptors and mediate anorectic effects of liraglutide in rats. *Sci. Transl. Med.* 12, eaay8071. <https://doi.org/10.1126/scitranslmed.aay8071>.
- Francis, J., Baer, L.A., Lehnig, A.C., Kawai, C., Emily, Y., Narain, and Niven, R. (2017). Lipidomic adaptations in white and Brown adipose tissue in response to exercise demonstrate molecular species-specific remodeling. *Cell Rep.* 18, 1558–1572. <https://doi.org/10.1016/j.celrep.2017.01.038>.
- Fruhbeck, G., Mendez-Gimenez, L., Fernandez-Formoso, J.A., Fernandez, S., and Rodriguez, A. (2014). Regulation of adipocyte lipolysis. *Nutr. Res. Rev.* 27, 63–93. <https://doi.org/10.1017/S095442241400002X>.
- Gabery, S., Salinas, C.G., Paulsen, S.J., Ahnfelt-Ronne, J., Alanentalo, T., Baquero, A.F., Buckley, S.T., Farkas, E., Fekete, C., Frederiksen, K.S., et al. (2020). Semaglutide lowers body weight in rodents via distributed neural pathways. *JCI Insight* 5, e133429. <https://doi.org/10.1172/jci.insight.133429>.
- Grzybek, M., Palladini, A., Alexaki, V.I., Surma, M.A., Simons, K., Chavakis, T., Klose, C., and Coskun, U. (2019). Comprehensive and quantitative analysis of white and brown adipose tissue by shotgun lipidomics. *Mol. Metab.* 22, 12–20. <https://doi.org/10.1016/j.molmet.2019.01.009>.
- Han, X. (2016). Lipidomics for studying metabolism. *Nat. Rev. Endocrinol.* 12, 668–679. <https://doi.org/10.1038/nrendo.2016.98>.
- Hishikawa, D., Hashidate, T., Shimizu, T., and Shindou, H. (2014). Diversity and function of membrane glycerophospholipids generated by the remodeling pathway in mammalian cells. *J. Lipid Res.* 55, 799–807. <https://doi.org/10.1194/jlr.R046094>.
- Hoffstedt, J., Arner, E., Wahrenberg, H., Andersson, D.P., Qvist, V., Lofgren, P., Ryden, M., Thorne, A., Wiren, M., Palmer, M., et al. (2010). Regional impact of adipose tissue morphology on the metabolic profile in morbid obesity. *Diabetologia* 53, 2496–2503. <https://doi.org/10.1007/s00125-010-1889-3>.
- Hou, B., Zhao, Y., He, P., Xu, C., Ma, P., Lam, S.M., Li, B., Gil, V., Shui, G., Qiang, G., et al. (2020). Targeted lipidomics and transcriptomics profiling reveal the heterogeneity of visceral and subcutaneous white adipose tissue. *Life Sci.* 245, 117352. <https://doi.org/10.1016/j.lfs.2020.117352>.
- Hu, S.Y., Zhang, Y., Zhu, P.J., Zhou, H., and Chen, Y.D. (2017). Liraglutide directly protects cardiomyocytes against reperfusion injury possibly via modulation of intracellular calcium homeostasis. *J. Geriatr. Cardiol.* 14, 57–66. <https://doi.org/10.11909/j.issn.1671-5411>.
- Huang, J.H., Chen, Y.C., Lee, T.I., Kao, Y.H., Chazo, T.F., Chen, S.A., and Chen, Y.J. (2016). Glucagon-like peptide-1 regulates calcium homeostasis and electrophysiological activities of HL-1 cardiomyocytes. *Peptides* 78, 91–98. <https://doi.org/10.1016/j.peptides.2016.02.007>.
- Kanoski, S.E., Hayes, M.R., and Skibicka, K.P. (2016). GLP-1 and weight loss: unraveling the diverse neural circuitry. *Am. J. Physiol. Regul. Integr. Comp. Physiol.* 310, R885–R895. <https://doi.org/10.1152/ajpregu.00520.2015>.
- Kolterman, O.G., Buse, J.B., Fineman, M.S., Gaines, E., Heintz, S., Bicsak, T.A., Taylor, K., Kim, D., Aisporna, M., Wang, Y., et al. (2003). Synthetic exendin-4 (exenatide) significantly reduces postprandial and fasting plasma glucose in subjects with type 2 diabetes. *J. Clin. Endocrinol. Metab.* 88, 3082–3089. <https://doi.org/10.1210/jc.2002-021545>.
- Krasner, N.M., Ido, Y., Ruderman, N.B., and Cacicco, J.M. (2014). Glucagon-like peptide-1 (GLP-1) analog liraglutide inhibits endothelial cell inflammation through a calcium and AMPK dependent mechanism. *PLoS One* 9, e97554. <https://doi.org/10.1371/journal.pone.0097554>.
- Lee, S.J., Sanchez-Watts, G., Krieger, J.P., Pignalosa, A., Norell, P.N., Cortella, A., Pettersen, K.G., Vrdoljak, D., Hayes, M.R., Kanoski, S.E., et al. (2018). Loss of dorsomedial hypothalamic GLP-1 signaling reduces BAT thermogenesis and increases adiposity. *Mol. Metab.* 11, 33–46. <https://doi.org/10.1016/j.molmet.2018.03.008>.
- Leech, C.A., Holz, G.G., and Habener, J.F. (1996). Signal transduction of PACAP and GLP-1 in pancreatic b cells. *Ann. N.Y. Acad. Sci.* 805, 81–92. <https://doi.org/10.1111/j.1749-6632.1996.tb17475.x>.
- Leiria, L.O., and Tseng, Y.H. (2020). Lipidomics of brown and white adipose tissue: implications for energy metabolism. *Biochim. Biophys. Acta Mol. Cell Biol. Lipids* 1865, 158788. <https://doi.org/10.1016/j.bbalip.2020.158788>.
- Lopez, M., Dieguez, C., and Nogueiras, R. (2015). Hypothalamic GLP-1: the control of BAT thermogenesis and browning of white fat. *Adipocyte* 4, 141–145. <https://doi.org/10.4161/21623945.2014.983752>.
- Lynch, L., Hogan, A.E., Duquette, D., Lester, C., Banks, A., LeClair, K., Cohen, D.E., Ghosh, A., Lu, B., Corrigan, M., et al. (2016). iNKT cells induce FGF21 for thermogenesis and are required for maximal weight loss in GLP1 therapy. *Cell Metab.* 24, 510–519. <https://doi.org/10.1016/j.cmet.2016.08.003>.
- Lyseng-Williamson, K.A. (2019). Glucagon-like peptide-1 receptor agonists in type 2 diabetes: their use and differential features. *Clin. Drug Invest.* 39, 805–819. <https://doi.org/10.1007/s40261-019-00826-0>.
- Marcher, A.-B., Loft, A., Nielsen, R., Vihervaara, T., Madsen, J.G.S., Sysi-Aho, M., Ekroos, K., and Mandrup, S. (2015). RNA-seq and mass-spectrometry-based lipidomics reveal extensive changes of glycerolipid pathways in brown adipose tissue in response to cold. *Cell Rep.* 13, 2000–2013. <https://doi.org/10.1016/j.celrep.2015.10.069>.
- Meier, J.J. (2012). GLP-1 receptor agonists for individualized treatment of type 2 diabetes mellitus. *Nat. Rev. Endocrinol.* 8, 728–742. <https://doi.org/10.1038/nrendo>.
- Merino, J., Leong, A., Liu, C., Porneala, B., Walford, G.A., Grothuss, M.v., Wang, T.J., Flannick, J., Dupuis, J., Levy, D., et al. (2018). Metabolomics insights into early type 2 diabetes pathogenesis and detection in individuals with normal fasting glucose. *Diabetologia* 61, 1315–1324. <https://doi.org/10.1007/s00125-018-4599-x>.
- Morigny, P., Boucher, J., Arner, P., and Langin, D. (2021). Lipid and glucose metabolism in white adipocytes: pathways, dysfunction and therapeutics. *Nat. Rev. Endocrinol.* 17, 276–295. <https://doi.org/10.1038/s41574-021-00471-8>.
- Noyan-Ashraf, M.H., Momen, M.A., Ban, K., Sadi, A.M., Zhou, Y.Q., Riaz, A.M., Baggio, L.L., Henkelman, R.M., Husain, M., and Drucker, D.J. (2009). GLP-1R agonist liraglutide activates cytoprotective pathways and improves outcomes after experimental myocardial infarction in mice. *Diabetes* 58, 975–983. <https://doi.org/10.2337/db08-1193>.
- Orskov, C., Wettergren, A., and Holst, J.J. (1996). Secretion of the incretin hormones glucagon-like peptide-1 and gastric inhibitory polypeptide

correlates with insulin secretion in normal man throughout the day. *Scand. J. Gastroenterol.* 31, 665–670. [https://doi: 10.3109/00365529609009147](https://doi.org/10.3109/00365529609009147).

Page, M.M., and Johnson, J.D. (2018). Mild suppression of hyperinsulinemia to treat obesity and insulin resistance. *Trends Endocrinol. Metab.* 29, 389–399. [https://doi: 10.1016/j.tem.2018.03.018](https://doi.org/10.1016/j.tem.2018.03.018).

Parveen, F., Bender, D., Law, S.H., Mishra, V.K., Chen, C.C., and Ke, L.Y. (2019). Role of ceramidases in sphingolipid metabolism and human diseases. *Cells* 8, 1537. [https://doi: 10.3390/cells8121573](https://doi.org/10.3390/cells8121573).

Raubenheimer, P.J., Nyirenda, M.J., and Walker, B.R. (2006). A choline-deficient diet exacerbates fatty liver but attenuates insulin resistance and glucose intolerance in mice fed a high-fat diet. *Diabetes* 55, 2015–2020. [https://doi: 10.2337/db06-0097](https://doi.org/10.2337/db06-0097).

Razquin, C., Toledo, E., Clish, C.B., Ruiz-Canela, M., Dennis, C., Corella, D., Papanicolaou, C., Ros, E., Estruch, R., and Guasch-Ferré, M. (2018). Plasma lipidomic profiling and risk of type 2 diabetes in the PREDIMED trial. *Diabetes Care* 41, 24. [https://doi: 10.2337/dc18-0840](https://doi.org/10.2337/dc18-0840).

Ronveaux, C.C., Tome, D., and Raybould, H.E. (2015). Glucagon-like peptide 1 interacts with ghrelin and leptin to regulate glucose metabolism and food intake through vagal afferent neuron signaling. *J. Nutr.* 145, 672–680. [https://doi: 10.3945/jn.114.206029](https://doi.org/10.3945/jn.114.206029).

Scheen, A.J., and Van Gaal, L.F. (2014). Combating the dual burden: therapeutic targeting of common pathways in obesity and type 2 diabetes. *Lancet Diabetes Endocrinol.* 2,

911–922. [https://doi: 10.1016/S2213-8587\(14\)70004-X](https://doi.org/10.1016/S2213-8587(14)70004-X).

Sun, F., Chai, S., Li, L., Yu, K., Yang, Z., Wu, S., Zhang, Y., Ji, L., and Zhan, S. (2015). Effects of glucagon-like peptide-1 receptor agonists on weight loss in patients with type 2 diabetes: a systematic review and network meta-analysis. *J. Diabetes Res.* 2015, 157201–157209. [https://doi: 10.1155/2015/157201](https://doi.org/10.1155/2015/157201).

Svensson, C.K., Larsen, J.R., Vedtofte, L., Jakobsen, M.S.L., Jespersen, H.R., Jakobsen, M.L., Koyuncu, K., Schjernin, O., Nielsen, J., Ekstrøm, C.T., et al. (2019). One-year follow-up on liraglutide treatment for prediabetes and overweight/obesity in clozapine- or olanzapine-treated patients. *Acta Psychiatr. Scand.* 139, 26–36. [https://doi: 10.1111/acps](https://doi.org/10.1111/acps).

Tao, L., Wang, L., Yang, X., Jiang, X., and Hua, F. (2019). Recombinant human glucagon-like peptide-1 protects against chronic intermittent hypoxia by improving myocardial energy metabolism and mitochondrial biogenesis. *Mol. Cell Endocrinol* 481, 95–103. [https://doi: 10.1016/j.mce.2018.11.015](https://doi.org/10.1016/j.mce.2018.11.015).

Topham, M.K. (2006). Signaling roles of diacylglycerol kinases. *J. Cell Biochem.* 97, 474–484. [https://doi: 10.1002/jcb.20704](https://doi.org/10.1002/jcb.20704).

Veilleux, A., Caron-Jobin, M., Noel, S., Laberge, P.Y., and Tchernof, A. (2011). Visceral adipocyte hypertrophy is associated with dyslipidemia independent of body composition and fat distribution in women. *Diabetes* 60, 1504–1511. [https://doi: 10.2337/db10-1039](https://doi.org/10.2337/db10-1039).

Viltsboll, T., Agerso, H., Krarup, T., and Holst, J.J. (2003). Similar elimination rates of glucagon-like peptide-1 in obese type 2 diabetic patients and

healthy subjects. *J. Clin. Endocrinol. Metab.* 88, 220–224. [https://doi: 10.1210/jc.2002-021053](https://doi.org/10.1210/jc.2002-021053).

Wang, Z.V., and Scherer, P.E. (2016). Adiponectin, the past two decades. *J. Mol. Cell Biol.* 8, 93–100. [https://doi: 10.1093/jmcb/mjw011](https://doi.org/10.1093/jmcb/mjw011).

Wei, Q., Li, L., Chen, J.-a., Wang, S., and Sun, Z.-l. (2015). Exendin-4 improves thermogenic capacity by regulating fat metabolism on Brown adipose tissue in mice with diet-induced obesity. *Ann. Clin. Lab. Sci.* 45, 158–165.

Xu, Z., You, W., Zhou, Y., Chen, W., Wang, Y., and Shan, T. (2019). Cold-induced lipid dynamics and transcriptional programs in white adipose tissue. *BMC Biol.* 17, 74. [https://doi: 10.1186/s12915-019-0693-x](https://doi.org/10.1186/s12915-019-0693-x).

Yang, A., and Mottillo, E.P. (2020). Adipocyte lipolysis: from molecular mechanisms of regulation to disease and therapeutics. *Biochem. J.* 477, 985–1008. [https://doi: 10.1042/BCJ20190468](https://doi.org/10.1042/BCJ20190468).

Zhang, F., Tang, L., Zhang, Y., Lu, Q., and Tong, N. (2017). Glucagon-like peptide-1 mimetics, optimal for Asian type 2 diabetes patients with and without overweight/obesity: meta-analysis of randomized controlled trials. *Sci. Rep.* 7, 15997. [https://doi: 10.1038/s41598-017-16018-9](https://doi.org/10.1038/s41598-017-16018-9).

Zhang, Y., Zhou, C., Li, X., Yang, M., Tao, L., Zheng, X., and Jia, Y. (2019). Beinaglutide showed significant weight loss benefit and effective glycemic control for the treatment of type 2 diabetes in a real-world setting: a 3-month, multicenter, observational, retrospective, open-label study. *Obes. Sci. Pract.* 5, 366–375. [https://doi: 10.1002/osp4.342](https://doi.org/10.1002/osp4.342).

## STAR★METHODS

## KEY RESOURCES TABLE

REAGENT or RESOURCE	SOURCE	IDENTIFIER
<b>Antibodies</b>		
Anti- $\beta$ -actin	Millipore Sigma	RRID:AB_476744
Phospho-Akt (Thr308) antibody	Cell Signaling	RRID:AB_329828
Phospho-Akt (Ser473) antibody	Cell Signaling	RRID:AB_329825
Akt antibody	Cell Signaling	RRID:AB_329827
Anti-uncoupling protein 1	Millipore Sigma	RRID:AB_91297
<b>Chemicals, peptides, and recombinant proteins</b>		
GLP-1	Cayman	15069
Beinaglutide	Shanghai Benemae Pharmaceutical Corporation	RN: 123,475-27-4
DPP IV inhibitor	EMD Millipore Corporation	DPP4-010
<b>Critical commercial assays</b>		
Milliplex TM Map kit	Merk milliplex	Cat. No. MADKMAG-71K
MAG single Plex kit	Merk milliplex	Cat. No. MADPNMAG-70K-01
<b>Deposited data</b>		
Sc-RNA seq raw data	This paper	GEO: PRJNA773225
<b>Experimental models</b>		
C57BL/6J	Slac Laboratory Animal Inc	NA

## RESOURCE AVAILABILITY

## Lead contact

Further information and requests for resources and reagents should be directed to and will be fulfilled by the lead contact Dr Fang Hu ([hu\\_fang98@csu.edu.cn](mailto:hu_fang98@csu.edu.cn)).

## Materials availability

This study did not generate new unique reagents.

## Data and code availability

The RNA-seq datasets generated during this study are available at NCBI Gene Expression.

Omnibus (GEO). Accession numbers are listed in the [key resources table](#).

Original code is available on Github: [https://github.com/zfjian/ISCI\\_103382](https://github.com/zfjian/ISCI_103382).

Any additional information required to reanalyze the data reported in this paper is available from the lead contact upon request.

## EXPERIMENTAL MODEL AND SUBJECT DETAILS

## Animals

Eight-week-old male C57BL/6J mice were purchased from Slac Laboratory Animal Inc. (Shanghai, China) and housed in a temperature-controlled environment (25°C) with a 12:12 h light/dark cycle and free access to food and water. Mice were fed an HFD (60 Kcal% fat, Cat #D12492; Research Diets Inc., New Brunswick, NJ) for 16 or 32 weeks to induce obesity. The GLP-1RA (150 ug/kg/day; Beinaglutide, CAS RN: 123,475-27-4; Shanghai Benemae Pharmaceutical Corporation, Shanghai, China) or vehicle solution administration was

performed through subcutaneous injections in the back three times a day for 6 weeks. The body weight and food intake of the mice were monitored weekly. After 6 weeks of drug treatment, animals were sacrificed. Fat depots and livers were rapidly removed and then immediately frozen in liquid nitrogen, and stored at  $-80^{\circ}\text{C}$  until further analysis.

For the *in vivo* insulin signaling study, mice fasted overnight, followed by an i.p. injection of insulin (5 units/kg body weight). Mice were sacrificed 5 min after the insulin injection, and tissues were harvested for further analyses.

For the cold tolerance test, obese mice treated with BN or vehicle were kept at room temperature ( $25^{\circ}\text{C}$ ) or in a cold chamber ( $6^{\circ}\text{C}$ ) for 4 h. In all groups, each mouse was maintained in a single cage with water and food. We evaluated the cold-induced thermogenesis by measuring the rectal temperature with a temperature sensor (AT210, Zhongyidapeng, Shenzhen, China).

All procedures involving animals were conducted in accordance with the guidelines set forth by the University Committee on the Care and Use of Animals of the Central South University, China.

## METHOD DETAILS

### Body composition, energy expenditure, and histological analysis

The body composition of the mice, including fat mass and lean mass, was determined using DEXA (GE Medical Systems, Madison, WI). Energy expenditure of the mice was determined by Oxymax/CLAMS metabolic cages (Columbus Instruments, USA) at standard room temperature conditions. The average oxygen consumption was normalized to lean body mass. Hematoxylin-eosin (H-E) staining and insulin and glucose tolerance experiments were performed according to our aforementioned procedures. After H-E staining, tissue slides were scanned with Quant Center2.1 (3Dhistech, Hungary). The diameters and areas of adipocytes were measured by Halo v3.0.311.314 (Indica Labs - Vacuole v2.2) and images were taken using a Nikon microscope (Eclipse TS100; Nikon, Tokyo, Japan).

### Cell culture and treatment

3T3-L1 adipogenesis were performed in DMEM supplemented with 100 U/mL penicillin, 100  $\mu\text{g}/\text{mL}$  streptomycin and 10% fetal bovine serum. Two days later when the fibroblasts had reached confluence, differentiation was induced by treating the cells with medium containing 3-isobutyl-1-methylxanthine, dexamethasone, and insulin for 48–72 h. And then were maintained in culture media mentioned above every other day for the next 4–6 days until more than 90% of cells demonstrating adipocyte phenotype. For treatment, 3T3-L1 and SVF-derived primary adipocytes were incubated with cell culture media containing DPP IV inhibitor (50  $\mu\text{M}$ , EMD Milipore Corporation, DPP4-010) to prevent BN degradation. After pre-treatment of BN (100 nM) or GLP-1 (100 nM; Cayman, Cat#15069) for 48 h, cells were cultured in fresh DMEM without FBS for 4 h. Insulin (10 nM) and BN or GLP-1 was added into DMEM for 5 min.

### RNA sequencing and analyses

For RNA isolation and library preparation, total RNA was extracted using the TRIzol reagent according to the manufacturer's protocol. RNA purity and quantification were evaluated using the NanoDrop 2000 spectrophotometer (Thermo Scientific, USA). RNA integrity was assessed using the Agilent 2100 Bioanalyzer (Agilent Technologies, Santa Clara, CA, USA). The libraries were constructed using TruSeq Stranded mRNA LT Sample Prep Kit (Illumina, San Diego, CA, USA) according to the manufacturer's instructions. The transcriptome sequencing and analysis were conducted by OE Biotech Co., Ltd. (Shanghai, China).

For RNA sequencing and differentially expressed gene analysis, the libraries were sequenced on an Illumina HiSeq X Ten platform and 150 bp paired-end reads were generated. Raw data (raw reads) of fastq format were first processed using Trimmomatic and the low-quality reads were removed to obtain the clean reads and the counts of each gene were obtained by HTSeqcount. Differential expression analysis was performed using the DESeq (2012) R package.  $p$  value  $<0.05$  and fold change  $>1$  or fold change  $<0.5$  was set as the threshold for significantly differential expression. GO enrichment and Functional enrichment analyses using the KEGG pathway enrichment analysis of DEGs were performed respectively using R based on the hypergeometric distribution.

### Western blotting

Samples of adipose tissues in lysis buffer with phospho-stop and proteinase inhibitor was centrifuged at 12,000 g for 5 min supernatant, and then was collected. Lysates were mixed in the 5×SDS protein sample loading buffer and heated to 100°C for 10 min. Samples were run on a 10% Bis-Tris criterion gel (Bio-Rad Laboratory Inc., Hercules, CA) at 80 volts for 30 min electrophoretic transferred at 120 V for 45–60 min. Primary antibodies was incubated for 16 h at 4°C, washed three times for each 10 min and then for second antibodies for 1 h in room temperature. Signals were detected using the ChemiDOCTMXRS+ and the Image Lab™ system (BIO-RAD, USA).

### Plasma lipid and hormone measurements

Blood samples were collected and centrifuged with 1000 g for 10 min at 4°C. The plasma levels of insulin and leptin were analyzed using a commercial mouse Milliplex™ Map kit (Cat. No. MADKMAG-71 K, USA), and adiponectin levels were analyzed using a mouse adiponectin MAG single Plex kit (Cat. No. MADPN-MAG-70K-01, USA). The following plasma lipids were measured including FFA, TG, total CHOL, HDL, LDL using Abbott Architect C8000 (Abbott Laboratories, USA). Abbreviations of lipids was shown in [Table S1](#).

### Adipose tissue lipid extraction

The lipid was extracted from 60 mg adipose tissue using 300 µL chloroform: methanol (2:1, v/v) contained isotope-labeled internal mix standards. The mixture was extracted using the ultrasonic method for 10 min and incubated at –20°C for 20 min. The chloroform layers were transferred into a centrifuge tube after centrifugation at 12,000 rpm and 4°C for 10 min. The second extraction was performed under the same conditions above. The combined chloroform layers of the two extractions were dried with a vacuum evaporator at 4°C. The samples were stored at 20°C for LC-MS analysis.

### Lipidomics analysis

Lipidomics profiling was conducted using a Dionex Ultimate 3000 UHPLC system fitted with Q-Exactive quadrupole-Orbitrap mass spectrometer via electrospray ionization (ESI) source (Thermo Fisher Scientific, Waltham, MA, USA). An ACQUITY UPLC BEH C18 column (1.7 µm, 2.1 × 100 mm) was employed in both positive and negative modes. The binary gradient elution system consisted of A (acetonitrile: water (60:40, v/v) plus 10 mmol/L ammonium formate) and B (acetonitrile: isopropanol (10:90, v/v) plus 10 mmol/L ammonium formate). The ESI ion source was set as follows: Heater Temp 350°C, Sheath Gas Flow rate 50 arb, Aux Gas Flow Rate 15 arb, Sweep Gas Flow Rate 1 arb, spray voltage 3.8 KV, Capillary Temp 320°C, S-Lens RF Level 75%. The resolution was set at 70,000 for the full MS scans and 17,500 for HCD MS/MS scans. The acquired raw data were analyzed by the LipidSearch software (Thermo Fisher Scientific, Waltham, MA, USA). The value of each sample represented the total peak area that was normalized for all peak signal intensity (peak area). The differential metabolites with normalized peak areas were selected based on the combination of a statistically significant threshold of variable importance of projection (VIP) values obtained from the OPLS-DA model. Metabolites with VIP values larger than 1.0 and *p* values less than 0.05 were considered as differential metabolites.

### QUANTIFICATION AND STATISTICAL ANALYSIS

All data were shown as mean ± SEM. Comparison between two groups were assessed using Student's two-tailed *t* test for independent samples and multiple groups were analyzed using one-way analysis of variance (ANOVA) (v19.0, SPSS Inc., Chicago, IL, USA). A *p* value less than 0.05 was considered to be statistically significant.